Idaho Department of Water Resources

Open File Report

FLUORESCENT DYE TRACER TESTS near Clear Lakes from the 'Ashmead' Well

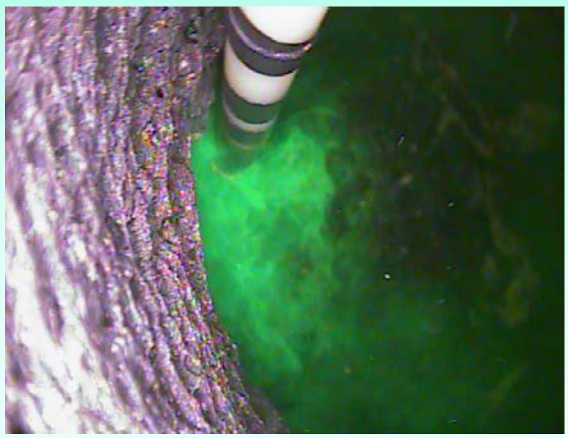

By

Neal Farmer
Idaho Department of Water Resources

and

David Blew
Idaho Power

February 18, 2014

ABSTRACT

Through an ongoing cooperative effort, between Idaho Power and the Idaho Department of Water Resources, two natural gradient dye tracer tests were conducted near Clear Lakes during the winter of 2012-2013 and a 3rd repeat trace in fall of 2013. Dye was injected into a domestic well 2,170 feet away from the springs and detected at several spring locations 15 to 17 hours later. Results document that groundwater is flowing generally from north to south at this location from the dye injection well to the springs. The dye break through response shows a single uni-modal curve with a near vertical rising limb and less steep but a high angle recession limb indicating a well constrained dye cloud. Trace #1 resulted in a maximum linear flow velocity of 2,976 feet per day based on the first arrival of dye and a dominant flow velocity of 1,653 feet per day based on the peak dye concentration. Trace #2 produced a maximum of 3,064 feet/day, dominant velocity of 1,602 feet/day, and an average velocity of 1,302 feet/day. Trace #3 was consistent with the previous 2 traces and documented a maximum velocity of 3,064 feet per day, a dominant flow velocity of 1,628 feet per day and 1,353 feet per day average. There have been no known previous traces performed in this area prior to year 2012. The tracer flow path is perpendicular to recent high resolution groundwater contour lines mapped in this area for the water table which demonstrates water is flowing down gradient and not tangent to the gradient. This report also presents a synoptic evaluation of recently gathered geologic information which sheds light on the significant role that older aged, brown colored basalts and sediments play with the aquifer in this area. An addition to this report is a table of data and information for all traces to date and interflow dye sample results, transverse, longitudinal and vertical dispersivity, and calculations for hydraulic conductivity as a substitute for obtaining conductivity values from traditional aquifer pumping tests.

TABLE OF CONTENTS

LIST OF ILLUSTRATIONS

INTRODUCTION AND BACKGROUND INFORMATION

The tracer tests presented in this report are an additional step for hydrologic studies of the East Snake Plain Aquifer (ESPA) and provide data and information for the application of practices to manage the aquifer. The tracing program also enhances the understanding of spring discharge, aquifer flow, geologic framework of the aquifer and a geologic history of the Snake River Plain. In a numerical groundwater model, two significant factors that affect model output are boundary conditions (how water flows into and out of a model) and hydraulic conductivity (K). Measuring and determining hydraulic conductivity is difficult on the ESPA, therefore as a substitute, tracer tests are helping fill the information gap by providing empirical field evidence of hydraulic conductivity. Provided in this report is a table listing the most recent data for all traces to date. This table contains updated values from improved GPS capabilities and supersedes previously reported values for data and calculations.

Figure 1 shows the location of dye injection for the ‘Ashmead’ trace next to the Clear Springs area. Data for this report was collected mostly within Township 9 South, Range 14 East, East ½ of Section 2, Gooding County. The methods, geography, well construction, tracing techniques, etc. are essentially the same as in previous traces south of Malad Gorge (Farmer and Blew, 2009, 2010, 2011). Previous authors provided evidence on factors that may control spring discharge from the ESPA such as ancient canyons on the Snake River plain that were filled and buried by volcanic eruptions (Stearns, 1936; Malde, 1971; Covington, 1985) and this same geologic model may also be present at Clear Springs area.

The Ashmead well (Tag #D0034163) was selected because it’s located immediately adjacent to the Clear Springs complex. High resolution groundwater contours also provided a basis for well selection and spring monitoring locations which indicated this well was directly up gradient from the main spring area. The water table map was generated through a cooperative effort between Idaho Power and Idaho Department of Water Resources during November 2011 and again in the fall of 2013. The dye injection well (Ashmead) meets new construction standards and it was completed to a depth of 60 feet below the water table and penetrates numerous permeable zones. It is a six-inch diameter domestic well completed in 2004 to a depth of 155 feet below land surface with a bottom hole elevation of 3,085 Ft. The casing extends to 18 feet below land surface and the well is open hole for the remainder of the well. The well was surveyed by Idaho Power using an RTK GPS base/rover method and Trimble R8 model. The elevation at the top of casing monitoring point is 3,240.20 feet. The water table at the time of the injection (Trace #1 & #2) was at an elevation of 3,144.7 or about 40 feet above the bottom of the well. There are no other wells between the injection well and the spring area.

A well camera, loaned by the U.S. National Park Service, was lowered down to inspect and document geologic conditions and the pump level. Grey colored basalt rock types dominated the full length of the well below the casing. Nearby deeper well logs suggest sediments and/or ‘brown’ colored basalt underlie the upper ‘grey’ basalt (Figures 2 & 3). Four deep wells were core drilled by an engineering firm in year 1991 (Chen-Northern, 1991), along with other more shallow monitor wells, prior to the cutting of the new Clear Lakes grade one mile east of the Ashmead well (Figure 3). The depths were 220, 250, 280 and 400 feet below land surface on the ESPA plateau. The geology was logged, core sampled and described by an engineer geologist.

Each well encountered clastic sediments at approximately 190 foot depth or 3,080-3,085 feet elevation which is a similar elevation as the bottom of the Ashmead well one mile west. The Ashmead well log noted cinders and the video camera showed a cavern in the bottom of the well with a strong downward flow of water observed in the well bore. This may be the upper geologic transition zone that grades into either the underlying ‘brown’ basalt or, if the brown basalt is absent at this location, then into the package of sediments identified from the Chen-Northern well logs and displayed as green and yellow patterns in Figure 3. The sediments in MW-2 were logged from 190 to 400 foot depth down to an elevation of 2,870 feet; with nearly 210 feet of continuous sediments under the basalt and the well terminates about 70 feet below the elevation of the Snake River. In-situ outcrop geology shows a brecciated cinder pillow basalt zone at the contact between the upper ‘grey’ basalt and the underlying ‘brown’ basalt (Figure 4). This zone could be what the Ashmead well encountered at 3,085 feet elevation.

Figure 5 shows three possible mega-scale geologic models for the geology near the Ashmead well and Clear Springs down to roughly the level of the river. The right column shows essentially the same geology exposed in outcrop at the Clear Springs highway road cut and the geology logged in monitor wells by Chen-Northern (1991). Since no ‘brown’ basalts were noted in the drillers log for the Ashmead well at the same elevation as the ‘brown’ basalts were encountered near the road cut, and since no ‘brown’ basalts were observed from the well video log, the left column may be more representative of the gross geology at Clear Springs area. The brown basalt was mapped by Gillerman et al. (2005), and it’s labeled as “Tb” meaning Tertiary age basalt. It appears to be a resistant erosional remnant of the ancient topography prior to deposits of the younger ‘grey’ colored Quaternary age basalt. It also appears to be discontinuous in nature and created localized highlands or mesas on the ancient topography along with Lake Idaho related sediments. This general concept and model was presented by previous researchers Stearns, 1936; Malde, 1971; Covington, 1985 and others.

A well shown in Figure 3 and labeled as “Clear Springs” was drilled in the canyon (Figure 2) and provides evidence of the underlying sediments encountered at approximately an elevation of 2,970 feet or approximately 50 feet above the river elevation. The thin basalt encountered in the upper 50 feet is likely remnants of the canyon wall toppling onto the valley floor from the Bonneville flood and/or this area may be an old landslide. The hydrogeologic conditions present are consistent with over 50 other landslides in the Hagerman Valley area. The Chen-northern report also notes this as a possible landslide area, therefore, the upper basalt encountered in the well is most likely landslide rubble from the overlying canyon wall and/or modified by the later Bonneville flood. Due to mechanics of landslide failures, the slip surface is likely at the elevation near the base of the canyon/river or higher. Therefore, the sediments encountered in the well below the rupture surface are likely in-situ which means there is a vast thickness of sediments below the Clear Springs area. The only sediments known with this thickness in the area are from the Glenns Ferry Formation. Geothermal waters and pressurized conditions likely exist under these sediments. There is good evidence the upper contact of these sediments extends northward based on the ‘Craig’ well (Figure 2 & 3), USGS ‘Henslee’ well, in-situ outcrops at Blind Canyon, Thousand Springs, south of Curren Tunnel, Vader Grade, numerous deep domestic wells near Vader Grade, in-situ outcrop at the mouth of Malad Gorge and the Bliss Grade. It is inferred the effective base of the upper cold ESPA aquifer at Clear Springs is the contact with these sediments at approximately 2,970 feet elevation based on the ‘Clear

Springs' well in Figure 3. This contact is undoubtedly undulatory in nature due to erosional processes prior to deposition of Quaternary age basalts and possibly augmented from landslides. If it is assumed that the contact is roughly at the level shown in the Clear Springs well at 2,970 feet and extending over to the Ashmead well, and using the elevation of the water level from the Ashmead well (3,144.7 feet), then an effective saturated aquifer thickness of 175 feet is equated near the Ashmead well.

A major control for groundwater movement in this area are sediments positioned below the host basalt of the ESPA that suggest a Glenns Ferry formation source. Some geologists have suggested that older less fractured brown Tertiary age basalts exposed in the valley (Figures 2, 3 and 4) are evidence of the effective base of the ESPA aquifer and that these more dense brown basalts extend to greater depths and possibly rest on top of Rhyolite basement rock. This is clearly not the case at the Clear Springs area where deep wells document that sediments appear to be the effective base of the upper cold water ESPA. Numerous springs located between the new road grade and the main Clear Springs area (Figure 2) have a low flow rate. Outcrop and Chen-Northern monitor well evidence supports they are discharging from below the Tertiary brown basalt and possibly flowing from sediments underneath the higher elevation basalts. There is an outcrop of the brown colored Tertiary age basalt located on the north side of the bridge that crosses the Snake River near Clear Springs (Figure 2). This outcrop is likely a displaced landslide block from higher elevations and the entire Clear Springs area is located on an ancient landslide. The US Army Corps of Engineers (1983 sec.2 pg. 2) state, "The ridge is considered to be either a slump block or an erosional remnant."

The brown Tertiary Basalts can have high permeability based on previous tracing results by Dallas, 2005; and Farmer and Larsen, 2001. These studies document high groundwater velocities within a Tertiary Age brown basalt that is interbedded within the Glenns Ferry Formation west of Hagerman but, this may not apply to the Tertiary Basalts near Clear Springs. It is sometimes assumed there are no grey colored basalts below the brown Tertiary Age basalt. But, grey basalts are described below the brown basalts by the Chen-Northern engineers report which recorded cores inspected by licensed Geoengineers (i.e. MW-2 Figure 3). Empirical field evidence supports, at least in part, that grey colored basalts are described below the brown basalts; it is concluded that the presence of Tertiary age basalts does not necessarily mean this is the base of the ESPA aquifer.

The USGS "Henslee" well west of Wendell at 07S14E35 SWSW (7 miles north of Clear Springs) also documents sediments shown in Farmer and Blew (2012, Figure 4). The elevation of sediments encountered in the Henslee well are positioned from 2,840 feet up to approximately 3,030 feet or about 190 foot thickness. The known sediments encountered at Clear Lakes grade range from at least 2,870 feet up to 3,080 feet for a thickness of at least 210 feet based on the Chen-Northern wells; and if the Clear Springs well is added then another 275 feet of sediments for a combined total thickness of approximately 500 feet of sediments. There are 600 feet of sediments exposed in outcrop at the Hagerman Fossil Beds National Monument. The difference in the upper contact elevation may be due to an apparent northerly dipping contact exposed in the road cut at the Clear Lakes grade trending downward to the north; or an undulating erosional paleo-surface; or both. More work on this is forthcoming in a subsequent report. The sediments at the Henslee well area function to separate the ESPA into an overlying basalt unconfined cold water table aquifer and an underlying partially confined warmer (72 degrees Fahrenheit) basalt aquifer.

Water is undoubtedly present and flowing through the course grained clastic sediments underneath the higher elevation less fractured brown basalt exhibited by the well logs and water levels from the Chen-Northern monitor wells discussed in the 1991 report which suggest saturated conditions within the sediments. Lower flow rate springs located just west of the Clear Springs highway grade and east of the Clear Springs/Lakes area are likely flowing from the sediments and may have a different chemical signature that is influenced by the sedimentary geology rather than the volcanic geology. The deepest well (MW-2 Figure 3) penetrated sediments from approximately 150 feet above the river elevation on down to the terminus of the well 70 feet below the elevation of the river. If a similar geology exists in the area of the Ashmead well, then the general Clear Lakes springs area might be a function of aquifer flow from both an upper basalt aquifer and underlying deeper clastic sediment aquifer. If this is correct then the two flow regimes may have two distinct chemical and physical signatures thus helping to explain chemical anomalies noted by Clear Springs.

Springs that daylight from the “R&D” facility at Clear Springs eastward past the Madalena springs to the new road grade area are vertically located within this zone of sediments identified by the monitor wells. The Chen-Northern (1991) report notes a shallow perched aquifer system on top of the old brown basalt, and this may be the system that has higher nitrate levels (DEQ, 2006) and flows laterally (probably northward given the apparent dip of the geologic contact) until merging/spilling into aquifer water to the north. This northward dipping contact, more dense Tertiary basalt, and underlying fine sediments of the Glenns Ferry Formation may account for the absence of springs eastward to Niagara Springs area. The influence of a northward dipping structure and low K basalts and sediments may induce a localized groundwater system along the rim area to have a northerly flow.

A well video shows that groundwater is flowing down the Ashmead well similar to other wells in the area south of the Malad Gorge. This vertical flow is likely not due to poor well construction but simply a strong downward gradient near the unconfined water table aquifer in spring discharge areas. Recent high resolution water table maps (Figure 6) show steep gradients in these areas, and dye trace results confirm high flow velocities associated with the steep gradients. Also, the mean flow paths are perpendicular to the gradient contours. Figure 6 shows wells and springs measured in the spring of 2013 and GPS’d as black circles for control of the contour lines which have 5 foot intervals and labeled every 25 feet. The red arrows show the direction of gradient. Figure 7 also shows the spring 2013 data as a 3-D water table surface map with contour lines at 5 foot intervals and feet units.

Figure 8 shows the steep water table map of the unconfined aquifer from the Ashmead well to the Clear Springs area and Figure 9 shows the projected water table between the well and spring CL-303 and the inferred dye trace profile. The top profile has a vertical exaggeration for clarification and the lower profile has a 1:1 ratio between vertical and horizontal distance. The blue line is simply drawn between the well water level and the spring elevation but the lower profile is from a modeled water table surface using ‘Surfer’ v. 11 software with the default ‘Kriging’ option selected which is an industry standard option and data contouring software.

The modeled grid surface metadata is shown in the appendix and the data source is from a mass synoptic groundwater measurement that occurred spring of 2013. The water table gradient is approximately 3% or 0.03 which drops 67 feet over a straight line distance of 2,170 feet. The dye injection elevation is plotted with a green square symbol on the left side axis of Figure 9 at 3,093 feet. Spring sample site CL-404, which had the highest concentration of dye, is approximately 29 feet lower in elevation than the bottom of the well where dye exited. Figure 9 shows how the modeled water table gradient is similar to the gradient between the dye exiting point out of the well and the spring with the greatest dye resurgence (CL-404). This supports that the main driving force of the dye is advective flow which is also roughly parallel to the hydraulic gradient.

A water level recorder was deployed in the Ashmead well on June 14, 2012 and programmed to record a measurement every 12 hours. Figure 10 shows the hydrograph over a period of about 1 year with a classic ESPA seasonal based cycle. The low or trough is during mid-July and a peak at approximately October 26th with a 4.5 foot seasonal water level change between the trough and peak. The rising limb of the hydrograph is much smoother, steady and a steeper rise than after it peaks and descends with a series of smaller scale cycles and a lower angle of recession or rate of decline. Roughly, the change in water level over approximately a 6 week period during the rising limb shows about a 2 to 2.5 foot increase verses a 6 week period during the recession limb of about 0.7 to 1 foot of water level decline. The two traces occurred during the period of December 13th through February 20th which the hydrograph shows some minor cycles on about a 15 day basis where the water levels are changing roughly ½ to 1 foot from peak to trough. For example on Jan. 10th the water level started to rise from a trough up by 0.82 feet to a peak on Jan. 16th, then lowered back to the next trough on the 26th. This frequency, magnitude and longer term trend was present during both traces #1 and #2 but the head change of approximately 0.5 to 0.8 feet is insignificant for effects to the traces given the travel distance verses gradient change from the well to the spring area. For example, the difference of 0.3 feet equates to a gradient change over 2,170 feet of 0.0001. It is unknown why these minor cycles are expressed after the seasonal peak during the recession limb but they are noticeably less so before the peak during the rising limb.

TRACING PROCEDURE AND METHODS

Trace #1 Description

Pre-trace data was collected at the springs to record natural background fluorescent noise. Water samples, charcoal detectors and a C3 Fluorometer were placed and submitted to a private lab for analysis. The lab results show no Fluorescein was detected in the spring water prior to dye injection from both the water samples and charcoal packets. Data from the C3 Fluorometer showed some natural background “noise” or interference which was a factor in calculating the mass of dye to release in order to have discernible and high confidence results for the dye breakthrough curve.

On December 13, 2012, two pounds of Fluorescein dye mixed with 4 gallons of drinking water was injected through polyethylene tubing at a depth of 147 feet below the top of the casing or elevation of 3,093.2 feet. Injection started at 11:18 am and by 11:29 am the injection was completed with 3.5 gallons of rinse water. The injection was video recorded and it showed a strong flow down and out the bottom of the well. A water sample was collected from the Ashmead well 2 hours after the injection of dye and submitted for analysis of total Coliform bacteria from a local lab with a result of “absent” for the presence of bacteria.

Figure 1 shows the location of the dye injection well which is approximately 2,170 feet from the Clear Lakes spring area in a straight line distance. The green arrow points to the spring with the highest concentration of dye following the injection. The red circles are locations where either charcoal detectors, instruments, grab samples or real time measurements were collected. The reader is cautioned regarding assumptions about the spring distribution due to modified and complex water routing through ditches, dikes, pipes, gates etc. Figure 11 helps clarify some of the routing with light blue lines and arrowheads showing some main flow paths of spring water through the diversion works. Spring sample sites are shown with red circles and identified as CL-100 through CL-404. The spring complex is divided up into 4 areas of 100’s, 200’s, 300’s and 400’s, but these divisions are not necessarily due to any particular reason other than an attempt at field organization of sample sites and a standardized numbering system. The sites noted with red text are sites with instrumentation deployed at common water collection points and therefore the results are an integrated value of the local discharge and capture feature. Some sites for example, CL-301, were selected for convenience or safety reasons. CL-300 and 301 sample sites shown with a red circle are located downstream from the main spring discharge. This concept is important to note for interpretation of the results.

The values shown in parentheses’ on Figure 11 are the dye concentration from charcoal detectors for trace #1. The results are charted in Figure 12 and listed in Table 1. The charcoal detectors were deployed from December 6th and retrieved on December 20th which is longer than the time of dye passage (3.5 days). The detectors were sent to the Ozark Underground Laboratory which specializes in dye tracing and analysis and has been used in previous dye tracing. Their lab equipment detects dye down to 0.002 parts per billion (2 parts per trillion) and ‘finger prints’ the chemical compound.

The CL-100 and 200 areas did not receive any detectable amounts of dye in the charcoal detectors nor in the instrument data but dye discharged in high concentrations from the CL-300 and 400 areas (Figure 12). Site CL-400 had the highest charcoal detector value of 1,120 parts per billion Fluorescein. Site CL-400 is a cement collection box for spring water that is captured from CL-404 and CL-405 and piped to CL-400 where it mixes together so the results from this location are an integration of the two springs. Figure 11 and the graph in Figure 12 show a decreasing dye concentration trend lateral and distant to spring sample site CL-404 (an inferred value has been added for site CL-404). The transverse dispersion of dye at the spring complex appears to be constrained based on a sharp delineation of dye at the margins; for example CL-203 had no detection of dye whereas site CL-300 had 14.9 ppb of dye. The east side of the dye resurgence was also contrasting where site CL-400 was 1,120 ppb and the adjacent site CL-402 was 1.47 ppb. The effective horizontal lateral dispersion of the dye resurgence is approximately 600 feet from the capture ditch of CL-300 to CL-402 over a linear flow path distance of 2,170.

The C3 fluorometer placed at site CL-400 collection box recorded a combined dye concentration from two springs that are piped into the cement box (Figure 13) with hourly frequency. It shows pre-injection noise in the data set on about December 12th but a clear first arrival of dye and peak with a partial recession limb. Unfortunately on December 15th until the 20th, due to a malfunction most of the recession limb data was lost for this site. The dye concentration breakthrough curve shows a near vertical rising limb with a sharp peak at 3.6 ppb then a sharp drop which indicates a well constrained longitudinal dispersion character. The maximum flow velocity based on the first arrival of dye and a straight line distance from the well to the sample site equates to a value of 2,976 feet per day and the dominant flow velocity based on the peak equates to a value of 1,653 feet per day. Consistent with previous tracer test data, the actual value calculated is reported without regard to significant figures. Onsite 'grab' sampling during the peak of the dye trace at the spring site CL-404 showed a peak dye concentration in the water of 6 ppb where the collection box at site CL-400 was 3.6 ppb. Despite the low level concentration of the resurgent dye, it was visible to the unaided eye at several sampling locations.

The C3 fluorometer placed at site CL-300 also showed a lower peak concentration of approximately 0.06 ppb (Figure 14) but a vertical shift of 0.01 was encountered for unknown reasons but related to the calibration process. This means the peak concentration at this site could have been lower at 0.05 ppb. Note the classic breakthrough curve shape with a steep rising limb, single peak, and lower angle recession limb which suggests a single flow path and well constrained slug of dye. The 'stepped' appearance of the curve is due to the very low concentrations that approach the detection limit and resolution of the instrument which is reported by the manufacturer as 0.01 ppb. The dye time of passage for this site is 48 hours. No dye was detected in the charcoal detectors for site CL-200 and the data from the C3 instrument showed only background noise or fluorescent interference (Figure 15). The charcoal packet at CL-200 also showed no dye passing through the sampling location.

Trace #2 Description

A second trace was completed using the same injection methods as the first trace but one pound less of Fluorescein or 50% reduced mass of dye. Two instruments were placed at spring site CL-404 and no other instruments or charcoal detectors at any other sites. The instruments included a C3 model and a newly designed model from the same manufacturer named the Cyclops 7 Logger that uses the same sensor as the C3. The Cyclops 7 logger was on loan from the manufacturer for field testing and evaluation based upon the authors previous tracing experience.

One pound of 75% concentration powder form dye was mixed with 4 gallons of potable water. The source of the dye purchased is the same as in all previous traces. Injection started on January 31, 2013 at 12:25 pm then 2.5 gallons of rinse water was injected. The two fluorometers were calibrated using store bought spring water for a blank and a 10 ppb solution purchased from the manufacturer. Based on the Cyclops 7 data shown as the blue data set in Figure 16, the first arrival of dye occurred 17 hours later on February 1 at approximately 5:30 am which equates to a maximum groundwater velocity of 3,064 feet per day. The C3 experienced background interference in the data set at the time of dye arrival which is seen as a 'spike' of the red colored data set in Figure 16 on about February 1st and then sudden significant drop back down to a trend matching the Cyclops 7. The rising limb data from both instruments match temporally and have essentially the same rate of increase or angle of graph on the rising limb concentration. The peak concentration from the Cyclops instrument occurred on February 1, at 9 pm or 32.5 hours after the time of dye injection at 2.6 ppb which equates to 1,602 feet per day for a dominant flow velocity. The Cyclops 7 experienced a battery failure and a loss of further data collection at 4:25 on February 2.

Both instruments recorded peak dye concentrations that were consistent for timing but the C3 had a value of about 2.1 ppb or about 0.5 ppb less than the Cyclops. It is believed, based on discussions with the manufacturer, the reason is a different focal length between the two instruments design based on the users application method. It is thought that the Cyclops 7 had the most accurate calibration and it correlates with a grab water sample analyzed using a lab fluorometer TD700 shown in Figure 16 with a green square symbol. An adjustment will be made on subsequent deployments and calibration procedures for the C3 units. A grab water sample was also sent to OUL lab for analysis and tested with different types of equipment that finger prints the chemical species with a result of 4.25 ppb Fluorescein.

The recession limb of data from the C3 appears consistent and reasonable until more interference cycles interrupt the trend with the same pattern that is clearly shown on about February 10. The abnormal patterns have been observed in the Malad Gorge traces from C3 data as well. This interference was also seen in some pre-test sampling at the springs. Water and charcoal detector samples from the periods of interference observed on a C3 were sent to the Ozark Underground Labs and tested negative for Fluorescein. The final break through curve was interpolated from February 3rd until February 9th. The lowest concentration data points were retained as control and the abnormal cycles removed during the late data recession. Then interpolated data was filled in between the control data points to generate a complete breakthrough curve shown in Figure 17. When this graph is compared to the breakthrough curve from Trace #1 it is consistent with a similar shape and zero background levels. It is also consistent with a 3rd trace performed a year later that produced complete results with no noise issues. The mean was calculated using the combined data sets from the Cyclops 7 and C3 along with filtered late data and then interpolated to fill in the trend to create a breakthrough curve for Trace #2 which is displayed as a yellow triangle in Figure 17 and calculates to a value of 1,302 feet per day for an average groundwater velocity and a time of passage of approximately 5 days.

Trace #3 Description

A third trace was performed from the Ashmead well on October 25, 2013 (one year after Trace #1 and #2) in order to refine the breakthrough curves from trace #2. The mass of dye was reduced by 50% to ½ pound of powder form (75% concentration) from trace #2 and mixed with 4 gallons of potable water to equal the same volume as the previous traces. Injection was video recorded and dye released at the same level in the well. Dye injection started at 10:54 am and completed at 10:57 am. C3 instruments were placed at spring site CL-404 and a common collection point for both of the drinking water springs CL-302 and 303. No other sites were monitored during this trace. Instruments were calibrated with purchased spring water for the blank and 10 ppb Fluorescein solution standard secured from the manufacturer. The instruments were programmed to record a reading on an hourly frequency. Figure 18 shows a clean (i.e.-no background noise) single peak unimodal positive skew dye concentration breakthrough curve from spring site CL-404. The peak concentration was measured at 1.35 ppb FL and the mean was calculated to be between two data points shown with two yellow diamond symbols.

The following list describes points on the curve in Figure 18:

1. Oct. 25, 10:57 am (blue diamond) – ½ pound FL mixed into 4 gallons injected.
2. Oct. 26, 3:30 am (green diamond) – first arrival of dye 17 hours (0.7 days).
3. Oct. 26, 18:30 pm (pink diamond) – peak concentration 32 hours (1.3 days).
4. Oct. 27, 1:00 am (yellow diamond) – mean concentration 38.5 hours (1.6 days).
5. The time of dye passage is approximately 98 hours or 4 days.

The straight line distance between the point of injection and CL-404 spring is 2,170 feet based on GPS and GIS methods therefore the maximum velocity based on the first arrival is 3,064 feet/day. The dominant velocity based on the peak concentration is calculated at 1,628 feet/day and the average linear velocity based on the mean is 1,353 feet/day. High velocities from this trace and other longer distance traces document groundwater flowing approximately an order of magnitude faster than noted on page 15 of the 2006 DEQ report by Baldwin and others and their modeling data noted on page 2. In addition, it appears from preliminary results of a current 3.5 mile trace from the Strickland well that water flowing west to Banbury spring and Briggs spring at a maximum rate of 771 feet per day and dominant flow velocity of 561 feet per day. Therefore the flow path may have a slightly different direction than the extreme west end of a flow system line (pink) in Figure 4 and Figure 10 of Schorzman and others (2009). The TOT in Figure 10 (Schorzman and others, 2009) may need to be recalculated for the capture zone based on current and future dye tracing data.

Figure 19 shows the dye breakthrough curve for the drinking water springs (CL-302 & 303) that are about 10 feet apart above the main access county road. These springs are the highest elevation springs along this immediate area. The water from both of these springs is captured and routed into the fish hatchery. There is a noise event prior to the release of dye on about October 24th. These noise events have been observed, monitored and tested for in previous traces by collecting water samples and sampling with charcoal packets and analyzed at private labs. Results have shown no dye during these noise events which means they are caused by something other than dye. The noise events always have peculiar shapes in the data set that are not typical of a chemical compound flowing in the water. For example, a typical response shows the data fluctuating from near zero values rising to high spikes then a vertical drop back to zero which is not typical of a dye flow pattern and easy to discern with experience and confirmation with lab testing. Figure 19 shows a blue diamond which is the time and date of dye injection, then a green diamond for first arrival of dye, pink diamond is the peak concentration at 0.08 ppb and the yellow diamond is the mean calculation. Figure 20 shows a plot of both C3 dye breakthrough curves for comparison with a running time since injection (t_0) in hourly units. The first arrival of dye in CL-302 & 303 site was delayed by 2 to 3 hours as compared to site CL-404 but the peaks of both curves occur at about the same time. Lower concentrations of dye which can't be detected until the threshold value of 0.01 is reached for the instrument to record a value may be the reason for the delayed first arrival. The two data sets have similar timing, shape, skew and a single peak and both peaks occur at essentially the same time.

DISCUSSION

The spatial information from Trace #1 combined with time of travel from trace #2 and #3 supports a highly conductive flow path between the well and the spring area. A composite breakthrough curve from Trace #2 was used to calculate the groundwater water velocities which are consistent with velocities from Trace #3 and the Malad Gorge traces. A single peak concentration of 2.6 ppb FL from Trace #2 demonstrates a unimodal breakthrough curve indicating a single dye flow path field with a sharp rising limb and typical lower angle recession limb. Trace #3 showed the same characteristics. Pre-test data showed no presence of dye prior to injection of Fluorescein but the instruments recorded some noise events which made breakthrough curve interpretation difficult requiring a large mass of dye used for the first 2 traces in order to overwhelm the background noise. The dye spread horizontally by approximately 600 feet over a linear distance of 2,170 feet but this spring complex has had a lot of manmade alterations which makes interpretation more difficult. The Ashmead traces provided maximum ground water velocities of 2,976, 3,064 and 3,064 feet per day. The dominant flow velocities were 1,653, 1,602 and 1,628 feet per day and the average groundwater velocities are 1,302 and 1,353 feet per day.

Although these velocities are on the scale of ½ mile, they stand in contrast to a velocity of 110 feet per day for Clear Springs from Table 3 in Baldwin et. al., (2000), but this is probably a lumped integrated velocity over all of the modeled area. Other values listed in Table 3 page 14 for the Malad Gorge, Briggs and Banbury spring are also low (120-130 feet/day) compared to tracing results listed in Table 2 of this report. The DEQ report states that modeling by WhAEM produced “very high velocities (up to 180 feet per day)”. Tracing has shown that groundwater velocity is constantly accelerating towards the spring discharge areas (velocity is constantly increasing) so it is not accurate to use just one value of velocity in WhAEM modeling over an area to produce a Time of Travel (TOT) capture zones. It is typical that water quality issues and modeling are concerned about when the first arrival of a chemical will reach a receptor. If so, then maximum groundwater velocities should be used from tracing to assist with this type of modeling and a grid cell size should be smaller than ¼ mile in resolution. The current version of Modflow, Modflow USG, allows for unstructured grids to accommodate almost any grid cell geometry which allows for more accurate discretization of time and space.

The velocities obtained from tracing to date are considered minimum values and the true velocities are likely higher. One reason for this is the detection limit of the in-situ instruments which is 0.01 ppb, and dye could arrive but not be detected until the threshold of 0.01 is exceeded, and in practice several times this threshold because of natural background noise in the data. This concept would shift all trace breakthrough curves to the left which means the first arrival of dye would be sooner, the peak would be sooner and the mean would be sooner which would increase the calculated velocities. If in the future, field equipment were developed with a lower detection limit or, if analysis is done by a private lab with a detection limit of 0.002 ppb, then less dye would be needed to complete the trace, the calculated velocities will increase, and the distance that dye tracing is feasible and viable will extend significantly.

The tracing information from tests near Clear Springs in context with local outcrops, a review of nearby ground truthed well drilling logs and other researcher’s reports and publications (i.e.-

Stearns, 1936; Malde, 1971; Covington, 1985; USACE, 1983; Chen-Northern, 1991) show similar geology as the Malad Gorge area. An ancient canyon may have existed which could be a major control in the physical and chemical character and movement of groundwater to Clear Springs. Rubble, cavernous, brecciated zones of pillow basalts are associated with the basal level of the ancient canyons that cut into Glenns Ferry age sediments; creating high velocity mega-scale regional based channels that route and transport ESPA water to springs with high discharge rates. The thalwag or deepest level of these canyons is lower in elevation relative to the water table therefore, the lower elevation and high flow rate springs may be less impacted by land surface activities than higher elevation springs and springs that are lateral to the main points of discharge. There could be minor vertical mixing in the flow system so the effect is that even soluble chemical compounds that reach the aquifer may 'ride' along the water table elevation zone and are not mixed with deeper waters moving in the thalwag unless there is a 'short circuit' via deep uncased wells. When these waters daylight at spring locations, there should be a difference in chemistry because of the lack of vertical mixing between shorter flow path, upper water table zone chemistry and the longer flow path, deeper thalwag chemistry. Similar to wells traced south of Malad Gorge, it is interpreted that the Ashmead well has penetrated the upper level of a thick sequence of a highly conductive brecciated pillow deposit. A recent trace named "Strickland" indicates that flow paths to Clear Springs may come from the east somewhere between the canyon rim and about 1 mile north of the rim which is consistent with previous USGS studies delineating the ancient buried Snake River Canyons. A report on the Strickland Trace is forthcoming.

Two important variable inputs to a numerical groundwater model are the boundary conditions and hydraulic conductivity of the aquifer. The ESPA is a highly conductive aquifer which means it is difficult to perform aquifer pumping tests that stress the aquifer enough over a large area to be meaningful. This is where the more cost efficient dye tracing methods can provide field data in selected areas. Tracer tests now cover several miles distance which makes them available for possible input into numerical models. Hydraulic conductivity values can be approximated from the following equation and Table 2 shows a list of values from tracing efforts to date.

$$\mathbf{K=(P_e*V_{ave})/I}$$

<u>Where:</u>

Effective Porosity	P_e= 0.20 (from ESPAM)
Average Velocity	V_{ave} = 1,353 feet/day (from Ashmead trace)
Gradient	I = (3144.7 ft. - 3078 ft.)/2170 ft.
	(well water table elev.-highest visible spr. water elev.)/trace distance

If gradient is determined by the elevation of the highest visible spring water then 'K' is approximately 8,828 feet/day (Table 2). Table 2 shows how gradient plays a significant role in the conductivity equation. There has been much discussion about how to refine the visible elevation of the springs relative to the hypothetical "true" elevation of the spring discharge due to the concept that in a talus slope spring water is cascading through the talus unseen to the eye until it emerges at a lower elevation conceptualized in Figure 21. This is a problem that may never be solved but there are ways to deal with it effectively. For example, dye tracing from well to well would eliminate this problem. Also, if a well were drilled next to the edge of the canyon to identify the water table next to the talus slope then this would help. Another accepted approximation method is to use the elevation that is halfway between where spring water is observable (or water loving vegetation – i.e. cattails, reeds, Tamarisk) and the top of the talus slope. When the gradient difference (visible spring emergence elevation compared to 25 feet higher in elevation) is plotted against the trace distance it becomes asymptotic in nature and after about 1 mile distance and the rate of change decreases and its effects decrease.

Figure 21 shows an idealized concept of how water may move through talus boulders along the canyon walls. Undoubtedly, there are locations where the aquifer exits the in-situ basalt wall of the canyon that is covered by overlying talus boulders. Then aquifer water may cascade down through the boulder talus for an unknown vertical distance before flowing laterally and exiting the talus slope at a lower elevation and day-lighting where the water is visible. This possible phenomenon causes problems for defining the true elevation of spring discharge and creates problems developing accurate water table maps. Defining the depth, extent and slope of talus material at each spring is difficult resulting in conjecture on the true elevation of spring discharge. However, examples exist on the ESPA that could serve as analogs for understanding aquifer discharge elevations. Curren Tunnel was developed along the contact between the overlying basalts and underlying sediments where brecciated pillows occur and the elevation of the discharge is visible from in-situ uncovered geology. The springs below Curren Tunnel, and along the east side slopes of the Hagerman Valley, have little talus or overburden to obscure the discharge and the elevation of discharge is readily visible. Springs mainly discharge along the contact between the overlying basalts and the underlying sediments associated with the Glenns Ferry Formation. Slope overburden tends to be dominated by fine clastic sediments and loess based material with lesser percentage of basalt boulders.

The springs at Clear Lakes flow out of a soil filled talus slope just like the springs between Thousand Springs and Malad Gorge. Data from the Ashmead trace suggests there is no extensive cascading water through the talus although undoubtedly some is occurring. There is only an approximate difference of seven vertical feet from the bottom of the Ashmead well to where dye exited from springs CL-302 & CL-303 (drinking water springs). Since, fine clastic sediments were identified in nearby wells drilled by Chen-Northern, the sediments in the talus could be sourced from the underlying geology and a topical deposition of loess. This demonstrates the importance sediments play in the understanding of the distribution and character of springs.

K values from tracing can be used for defining aquifer properties and it should be noted that the values are integrated over the distance of the trace. For example: a dye velocity obtained from a 3 mile trace is the integrated value over that distance. Generally, velocity is constantly accelerating due to a constantly steepening water table gradient as it approaches the spring areas (Figure 22). Therefore, dye should be travelling relatively slow near the point of injection and constantly increases in velocity as it approaches the spring discharge area. Use of K values from tracing may help in strategic or selected near rim areas.

ACKNOWLEDGEMENTS
This project is supported with financial assistance and personnel from Idaho Power and the Idaho Department of Water Resources. Clear Springs Foods and the Homeowner's Association were very cooperative and instrumental for the success of the trace.

REFERENCES AND SOURCES OF INFORMATION

1. Aley, T., 2002, Groundwater tracing handbook, Ozark Underground Labs, 44 p.

2. Aley, T., 2003, Procedures and criteria analysis of Fluorescein, eosine, Rhodamine wt, sulforhodamine b, and pyranine dyes in water and charcoal samplers, Ozark Underground Labs, 21 p.

3. Anderson, M.P., 2005, Heat as a ground water tracer, Ground Water Journal, November-December, Vol. 43, No. 6, pages 951-968.

4. Anderson, M. P. and Woessner, W. W., 1992, Applied groundwater modeling, Academic Press, San Diego.

5. Anderson, M.P., 1979, Using models to simulate the movement of contaminants through groundwater flow systems, Critical Reviews in Environmental Controls 9, no. 2: 97-156.

6. Aulenbach, D.B., Bull, J.H., and Middlesworth, B.C., 1978, Use of tracers to confirm ground-water flow: Ground Water, Vol. 16, No. 3, 149-157 p.

7. Axelsson, G., Bjornsson, G., and Montalvo, F., 2005, Quantitative interpretation of tracer test data, Proceedings World Geothermal Congress, 24-29 p.

8. Baldwin, J., Brandt, D., Hagan, E., and Wicherski, B., 2000, Cumulative impacts assessment, Thousand Springs area of the eastern snake river plain Idaho, Department of Environmental Quality, Ground Water Quality Technical Report No. 14, 56 p.

9. Baldwin, J., Winter, G., and Dai, Xin, 2005 update, thousand springs area of eastern snake plain Idaho, Department of Water Quality, Ground Water Quality Technical Report No. 27, 2006, 73 p.

10. Bonnichsen, B., and Godchaux, M.M., 2002, Late Miocene, Pliocene, and Pleistocene Geology of Southwestern Idaho With Emphasis on Basalts in the Bruneau-Jarbidge, Twin Falls, and Western Snake River Plain Regions; Tectonic and Magmatic Evolution of the Snake River Plain Volcanic Province, Idaho Geological Survey, Bulletin 30, 482 p.

11. Bonnichsen, B., McCurry, M., and White, C.M., 2002, Tectonic and Magmatic Evolution of the Snake River Plain Volcanic Province, Idaho Geological Survey Bulletin 30, 482 p.

12. Bowler, P.A., Watson, C.M., Yearsley, J.R., Cirone, P.A., 1992, Assessment of ecosystem quality and its impact on resource allocation in the middle Snake River sub- basin; (CMW, JRY, PAC - U.S. Environmental Protection Agency, Region 10; PAB - Department of Ecology and Evolutionary Biology, University of California, Irvine), Desert Fishes Council (http://www.desertfishes.org/proceed/1992/24abs55.html).

13. Chen-Northern, Inc., 1991, Hydrogeologic assessment at Clear Lakes grade, Gooding county, Idaho, Idaho State Department of Transportation, Key # 03586 and Key # 05849, Boise Idaho State Street office, prepared by Paul Spillers, 44 p. plus appendices. (hard copy on file at IDWR).

14. Covington, H.R., and Weaver, J. N., 1991, Geologic maps and profiles of the north wall of the Snake river canyon, Thousand springs and Niagra springs quadrangles, Idaho, U.S. Geological Survey, Miscellaneous Investigation Series, Map I-1947-C.

15. Covington, H.R., Whitehead, R.L., and Weaver, J.N., 1985**,** Ancestral canyons of the Snake River; geology and geohydrology of canyon-fill deposits in the Thousand Springs area, south-central Snake River Plain, Idaho: Geological Society of America Rocky Mountain Section, 38th Annual Meeting, Boise, Idaho, 1985, Composite Field Guide, Trip 7, 30 p.

16. Crandall, L., 1918, The springs of the Snake River canyon, Idaho Irrigation, Engineering, and Agriculture Societies Joint Conference Proceeding, pp. 146-150.

17. Dallas, K., 2005, Hydrologic study of the Deer Gulch basalt in Hagerman fossil beds national monument, Idaho, thesis, 96 p.

18. Davies, G.J., 2000, Lemon lane landfill investigation, Technical Note: Groundwater tracing using fluorescent dyes: interpretation of results and its implications, The Coalition Opposed to PCB Ash in Monroe County, Indiana, 24 p.

19. Davis, S., Campbell, D.J., Bentley, H.W., Flynn T.J., 1985, Ground water tracers, 200 p.

20. Dole, R.B., 1906, Use of Fluorescein in the study of underground waters, pg 73, USGS Water Supply Paper, #160, series 0, Underground Waters, 58, by Fuller M.L., 104 p.

21. Domenico P.A. and Schwartz F.W., 1990, Physical and chemical hydrogeology, John wiley & sons, 824 p.

22. Enotes, 2011, web site address: http://www.enotes.com/earth-science/geothermal-gradient

23. Farmer N., and Blew D., 2011, Fluorescent dye tracer tests and hydrogeology near the Malad Gorge state park (Hopper well test), Idaho Department of Water Resources Open File Report, 41 p.

24. Farmer N., and Blew D., 2010, Fluorescent dye tracer tests near the Malad Gorge state park (Riddle well test), Idaho Department of Water Resources Open File Report, 36 p.

25. Farmer N., 2009, Review of hydrogeologic conditions located at and near the spring at Rangen inc., Idaho Department of Water Resources open file report, 46 p.

26. Farmer N., and Owsley, D., 2009, Fluorescent dye tracer test at the W-canal aquifer recharge site, Idaho Department of Water Resources Open File Report, 23 p.

27. Farmer N., and Blew D., 2009, Fluorescent dye tracer tests at Malad Gorge state park, Idaho Department of Water Resources Open File Report, 45 p.

28. Farmer N., 2008, Traffic jams occur in nature too – geologic architecture of Hagerman valley spring discharge areas, Idaho Water Resource Research Institute Ground Water Connections Conference, Sept. 23 & 24, Boise, Idaho, Session 4 Research.

29. Farmer N., and Kathren, R.L., 2008, Radioactivity in fossils at the Hagerman fossil beds national monument, Journal of Environmental Radioactivity, Aug; 99(8):1355-9.

30. Farmer, C.N., and Nagai, O., 2004, Non-native vegetation growth patterns as a tracer for development of human caused perched aquifers in landslide areas, Journal of the Japan Landslide Society, vol. 41, no. 3 (161), 12 p.

31. Farmer N., and Larsen, I., 2001, Ground water tracer tests at the Hagerman fossil beds national monument, unpublished U.S. Dept. of Interior, National Park Service technical report, January 2001, 21 p.

32. Farmer N., 1998, Hydrostratigraphic model for the perched aquifer systems located near Hagerman fossil beds national monument, Idaho, University of Idaho thesis, 106 p.

33. Fetter, C.W., 1988, Applied hydrogeology, second edition, Macmillan publishing company, 592 p.

34. Fetter, C.W., 1993, Contaminant hydrogeology, Macmillan publishing company, 458 p.

35. Faulds, J. E., and R. J. Varga, 1998, The role of accommodation zones and transfer zones in the regional segmentation of extended terranes, *in* J. E. Faulds and J. H. Stewart, eds., Accommodation zones and transfer zones: the regional segmentation of the Basin and Range province: Geological Society of America Special Paper 323, p. 1–46.

36. Field, M.S., Wilhelm R.G., Quinlan J.F. and Aley T.J., 1995, An assessment of the potential adverse properties of fluorescent tracer dyes used for groundwater tracing, Environmental Monitoring and Assessment, vol. 38, 75-96 p.

37. Gaikowski, M.P., Larson, W.J., Steuer, J.J., Gingerich, W.H., 2003, Validation of two dilution models to predict chloramine-T concentrations in aquaculture facility effluent, Aquacultural Engineering 30, 2004, 127-140 p.

38. Galloway, J.M., 2004, Hydrogeologic characteristics of four public drinking water supply springs in northern Arkansas, U.S. Geological Survey Water-Resources Investigations Report 03-4307, 68 p.

39. Gillerman, V.S., J.D. Kauffman and K.L. Othberg, 2005, Geologic Map of the Thousand Springs Quadrangle, Gooding and Twin Falls Counties, Idaho: Idaho Geological Survey digital web map 49.

40. Gillerman, V.S., J.D. Kauffman and K.L. Othberg, 2005, Geologic Map of the Tuttle Quadrangle, Gooding and Twin Falls Counties, Idaho: Idaho Geological Survey digital web map 51.

41. Gillerman, V.S., J.D. Kauffman and K.L. Othberg, 2005, Geologic Map of the Hagerman Quadrangle, Gooding and Twin Falls Counties, Idaho: Idaho Geological Survey digital web map 50.

42. Harvey, K.C., 2005, Beartrack mine mixing zone dye tracer study outfall 001, Napias creek Lemhi county, Idaho, Private Consulting Report by KC Harvey, LLC., 59 p.

43. Hudson, B.G. and Moran, J.E., 2002, Delineation of fast flow paths in porous media using noble gas tracers, U.S. Dept. of Energy Lawrence Livermore National Laboratory, CA., 18 p.

44. Kass, W. et. al., 2009, Tracing technique in geohydrology, reprinted by CRC Press from year 1998 publishers A.A. Balkema, 581 p.

45. Kilpatrick, F.A. and Cobb, E.D., 1985, Measurement of discharge using tracers, U.S. Geological Survey Techniques of Water-Resources Investigations Report, book 3, chapter A16.

46. Klotz, D., Seiler K.P., Moser H., and Neumaier F., 1980, Dispersivity and velocity relationship from laboratory and field relationships. Journal of Hydrology 45, no. 3: 169-84.

47. Kruseman G.P. and Ritter N.A., 1991, Analysis and evaluation of pumping test data, second edition, International institute for land reclamation and improvement, 377 p.

48. Leet, D., Judson, S. and Kauffman, M., 1978, Physical Geology, 5th edition, ISBN 0-13-669739-9, 490 p.

49. Leibundgut, C. and H. R. Wernli. 1986. Naphthionate--another fluorescent dye. Proc. 5th Intern'l. Symp. on Water Tracing. Inst. of Geol. & Mineral Exploration, Athens, 167-176 p.

50. Malde, H.E., 1991, Quaternary geology and structural history of the Snake River Plain, Idaho and Oregon in Morrison, R.B., ed., Quaternary nonglacial geology; conterminous U.S.: Boulder, CO, Geological Society of America, The Geology of North America, vol. K-2.

51. Malde, H.E., 1982, The Yahoo Clay, a lacustrine unit impounded by the McKinney Basalt in the Snake River canyon near Bliss, Idaho, in Bonnichsen, B., and Breckenridge, R.M., eds., Cenozoic geology of Idaho: Idaho Bureau of Mines and Geology Bulletin 26, p. 617-628.

52. Malde, H.E., 1972, Stratigraphy of the Glenns Ferry Formation from Hammett to Hagerman, Idaho: U.S. Geological Survey Bulletin 1331-D, 19 p.

53. Malde, H.E., 1971, History of Snake River canyon indicated by revised stratigraphy of Snake

River group near Hagerman and King Hill, Idaho, Shorter contributions to general geology; Geological Survey professional paper, 644-F, 21 p.

54. Malde, H.E., and Powers, H. A., 1958, Flood-plain origin of the Hagerman Lake Beds, Snake River Plain, Idaho (abs.): Geological Society of America Bulletin, v. 69, 1608 p.

55. Marking, L., Leif, 1969, Toxicity of Rhodamine b and Fluorescein sodium to fish and their compatibility with antimycin A, The Progressive Fish Culturist, vol. 31, July 1969, no. 3. 139-142 p.

56. McClay, K.R., Dooley, T., Whitehouse, P., and Mills, M., 2002, 4-D evolution of rift systems: Insights from scaled physical models, AAPG Bulletin, V. 86., no. 6 (June 2002), pp. 935-959.

57. Meinzer, O.E., 1927, Large springs in the United States, USGS Water Supply Paper 557, library number (200) G no.557, 94 p.

58. Moser, H., 1995, Groundwater tracing, Tracer Technologies for Hydrological Systems (Proceedings of a Boulder Symposium, July 1995), IAHS Publ. No. 229, 1995.

59. Mull, D.S., Liebermann, T.D., Smoot, J.L., Woosley, L.H. Jr., (U.S. Geological Survey), 1988, Application of dye-tracing techniques for determining solute-transport characteristics of ground water in karst terrranes; U.S. EPA904/6-88-001, 103 p.

60. Noga, E.J., and Udomkusonsri, P., 2002, Fluorescein: a rapid, sensitive, non-lethal method for detecting skin ulceration in fish, Vet Pathol 39:726–731 p.

61. Othberg, K.L. and Kauffman, J.D., 2005, Geologic map of the Bliss quadrangle, Gooding, and Twin Falls counties, Idaho, Idaho Geological Survey map #53.

62. Otz, M. H., and Azzolina, N.A., 2007, Preferential ground-water flow: evidence from decades of fluorescent dye-tracing, Geological Society of America fall meetings presentation, 19 slides.

63. Olsen, L.D. and Tenbus F.J., 2005, Design and analysis of a natural-gradient groundwater tracer test in a freshwater tidal wetland, west branch canal creek, Aberdeen proving ground, Maryland, U.S. Geological Survey Scientific Investigation Report 2004-5190, 116 p.

64. Parker, G.G., 1973, Tests of Rhodamine WT dye for toxicity to oysters and fish, Journal of Research U.S. Geological Survey, Vol. 1, No. 4, July-Aug., 499 p.

65. Putnam, L.D. and Long A.J., 2007, Characterization of ground-water flow and water quality for the Madison and minnelusa aquifers in northern Lawarence county, South Dakota, U.S. Geological Survey Scientific Investigation Report 2007-5001, 73 p.

66. Quinlan, J.F. and Koglin, E.N. (EPA), 1989, Ground-water monitoring in karst terrranes: recommended protocols and implicit assumptions, U.S. Environmental Protection Agency, EPA 600/x-89/050, IAG No. DW 14932604-01-0, 79 p.

67. Quinlan, J.F., 1990, Special problems of ground-water monitoring in karst terranes, Ground Water and vadose Zone Monitoring, ASTM STP 1053, D.M. Nielsen and A.I. Johnson, (Eds), American Society for Testing and Materials, Philadelphia, p. 275 -304.

68. Ralston, D., 2008, Hydrogeology of the thousand springs to Malad reach of the enhanced snake plain aquifer model, Idaho Department of Water Resources report, 20 p.

69. Russell, I.C., 1902, Geology and water resources of the Snake river plains of Idaho, USGS Bulletin 199, library number (200) E no.199, 192 p.

70. Schorzman, K., Baldwin, J., and Bokor, J., 2009, Possible sources of nitrate to the springs of southern Gooding county, eastern snake river plain, Idaho, Department of Environmental Quality, Ground Water Quality Technical Report No. 38, 41 p.

71. Shervais, J., Evans, J.P., Lachmar, T.E., Christiansen, E.J., Schmitt, D.R., Kessler, J.E., Potter, K. E., Jean, M.M., Sant, C.J., Freeman, T.G., Project hotspot – the Snake river scientific drilling project: a progress report, Geological Society of America Rocky Mountain 63rd Annual meeting and Cordilleran 107th Annual meeting May 18-20, 2011, Abstracts with Programs, Vol. 43, No. 4, p. 5.

72. Smart, C. and Simpson B.E., 2002, Detection of fluorescent compounds in the environment using granular activated charcoal detectors, Environmental Geology, vol. 42, 538-545 p.

73. Smart, P.L., 1984, A review of the toxicity of twelve fluorescent dyes used for water tracing, National Speleological Society publication, vol. 46, no. 2: 21-33.

74. Smart, P.L., 1984, A review of the toxicity of twelve fluorescent dyes used for water tracing, National Speleological Society publication, vol. 46, no. 2: 21-33.

75. Spangler, L.E., and Susong, D.D., 2006, Use of dye tracing to determine ground-water movement to Mammoth Crystal springs, Sylvan pass area, Yellowstone national park, Wyoming, U.S. Geological Survey Scientific Investigations Report 2006-5126, 19 p.

76. Stanovich, Keith E. (2007). How to think straight about Psychology. Boston: Pearson Education, 123 p.

77. Stearns, H.T., 1983, Memoirs of a geologist: from Poverty peak to Piggery gulch, Hawaii Institute of Geophysics, 242 p.

78. Stearns, H.T., Crandall, L., Steward, W.G., 1938, Geology and ground-water resources of the Snake River plain in southeastern Idaho; U.S. Geological Survey Water Supply Paper 774, 268 p.

79. Stearns, H. T., 1936, Origin of large springs and their alcoves along the snake river in southern Idaho, The Journal of Geology, vol. 44, No. 4, 429-450 p.

80. Taylor, C.J., and Greene E.A., Hydrogeologic characterization and methods used in the investigation of karst hydrology, U.S. Geological Survey field techniques for estimating water fluxes between surface water and ground water, chapter 3, Techniques and Methods 4-D2, 71-114 p.

81. Taylor, C.J., and Alley, W.M., 2001, Ground-water-level monitoring and the importance of long-term water-level data, U.S. Geological Survey Circular 1217, 68 p.

82. Turner Designs, Inc., A practical guide to flow measurement, www.turnerdesigns.com.

83. U.S. Army Corps of Engineers, 1983, Interim Feasibility Report – Clear Lakes Hydropower Snake River, Idaho, Upper Snake River and Tributaries, for Idaho Water Resource Board, 62 p. (original hard copy on file at IDWR)

84. U.S. Bureau of Reclamation Water Measurement Manual, 2001, http://www.usbr.gov/pmts/hydraulics_lab/pubs/wmm/

85. Walthall, W.K., and Stark J.D., 1999, The acute and chronic toxicity of two xanthene dyes, Fluorescein sodium salt and phloxine B, to Daphnia pulex, Environmental Pollution volume 104, 207-215 p.

86. Wilson, J.F., Cobb, E.D., and Kilpatrick F.A., 1986, Fluorometric procedures for dye tracing, U.S. Geological Survey Techniques of Water-Resources Investigations of the United States Geological Survey, Applications of Hydraulics, book 3, chapter A12, 43 p.

APPENDIX A – Miscellaneous Information

HYDROGEOLOGIC ASSESSMENT
AT CLEAR LAKES GRADE
FEDERAL-AID PROJECT RS-2709(006)
GOODING COUNTY, IDAHO

Prepared for:

Sharp and Smith Consulting Engineers and Surveyors
327 N. 27th Street
Boise, ID 83702

Prepared by:

Chen-Northern, Inc.
Boise, ID

October 1991

Idaho Dept. of Transportation, Boise Idaho, State Street office Key #'s 03586 and 05849.

Water Table Grid Information

Wed Oct 09 13:30:34 2013

Grid File Name:	D:\data\Dye Tracing\Mass Measurement\2013 Mass Meas\2011&2013_Water_Levels_Final.grd
Grid Size:	184 rows x 200 columns
Total Nodes:	36800
Filled Nodes:	17267
Blanked Nodes:	19533
Blank Value:	1.70141E+038

Grid Geometry

X Minimum:	7959026.849
X Maximum:	8079872.421
X Spacing:	607.26418090452
Y Minimum:	4161513.12
Y Maximum:	4272568.023
Y Spacing:	606.85739344262

Univariate Grid Statistics

	Z
Count:	17267
1%%-tile:	2996.44367704
5%%-tile:	3072.39366202
10%%-tile:	3120.21447422
25%%-tile:	3184.138812
50%%-tile:	3258.68017855
75%%-tile:	3313.05920118
90%%-tile:	3428.28029293
95%%-tile:	3494.36235945
99%%-tile:	3559.37440896
Minimum:	2948.97120431
Maximum:	3584.76542411
Mean:	3260.74346552
Median:	3258.68017855
Geometric Mean:	3258.64646869

Harmonic Mean:	3256.56193338
Root Mean Square:	3262.85323288
Trim Mean (10%%):	3258.48035385
Interquartile Mean:	3254.95880064
Midrange:	3266.86831421
Winsorized Mean:	3259.59968264
TriMean:	3253.63959257
Variance:	13764.0685521
Standard Deviation:	117.320367167
Interquartile Range:	128.920389177
Range:	635.794219807
Mean Difference:	129.982024541
Median Abs. Deviation:	65.7312825739
Average Abs. Deviation:	88.8574437563
Quartile Dispersion:	0.0198424596135
Relative Mean Diff.:	0.039862695706
Standard Error:	0.89282217642
Coef. of Variation:	0.0359796372844
Skewness:	0.339234949455
Kurtosis:	3.27239040799
Sum:	56303257.4191
Sum Absolute:	56303257.4191
Sum Squares:	183828129124
Mean Square:	10646211.2193

GPS Coordinates of Sample Sites in IDTM NAD83

- Collected using a Trimble ProXRT and GeoXT 2005 set at maximum precision for spring sites and RTK Trimble R8 for the well head.
- Easting and Northing units are in meters and elevation is in feet units.

Site_ID	Easting (m)	Northing (m)	Elevation (ft.)
Ashmead well	2436767.49	1275885.99	3240.20
CL-100	2436333.2	1275165.5	3033
CL-101	2436328.2	1275165.8	3036
CL-102	2436201.2	1275190.6	3063
CL-103	2436263.2	1275189.6	3063
CL-200	2436484.2	1275165.7	3041
CL-201	2436458.4	1275208.8	2918
CL-202	2436462.9	1275199.6	3032
CL-203	2436490.2	1275207.0	3031
CL-300	2436574.1	1275223.3	3043
CL-301	2436572.0	1275211.5	3034
CL-302	2436583.4	1275241.1	3078
CL-303	2436571.0	1275248.9	3078
CL-400	2436661.8	1275220.6	3055
CL-401	2436722.9	1275245.6	3061
CL-402	2436705.2	1275244.7	3058
CL-403	2436609.5	1275236.2	3043
CL-404	2436639.0	1275237.0	3056

Figure 1. Trace location map showing the injection well 2,170 feet straight line distance from the spring sample sites with red circles. Green arrow head line denotes the spring with the highest dye concentration.

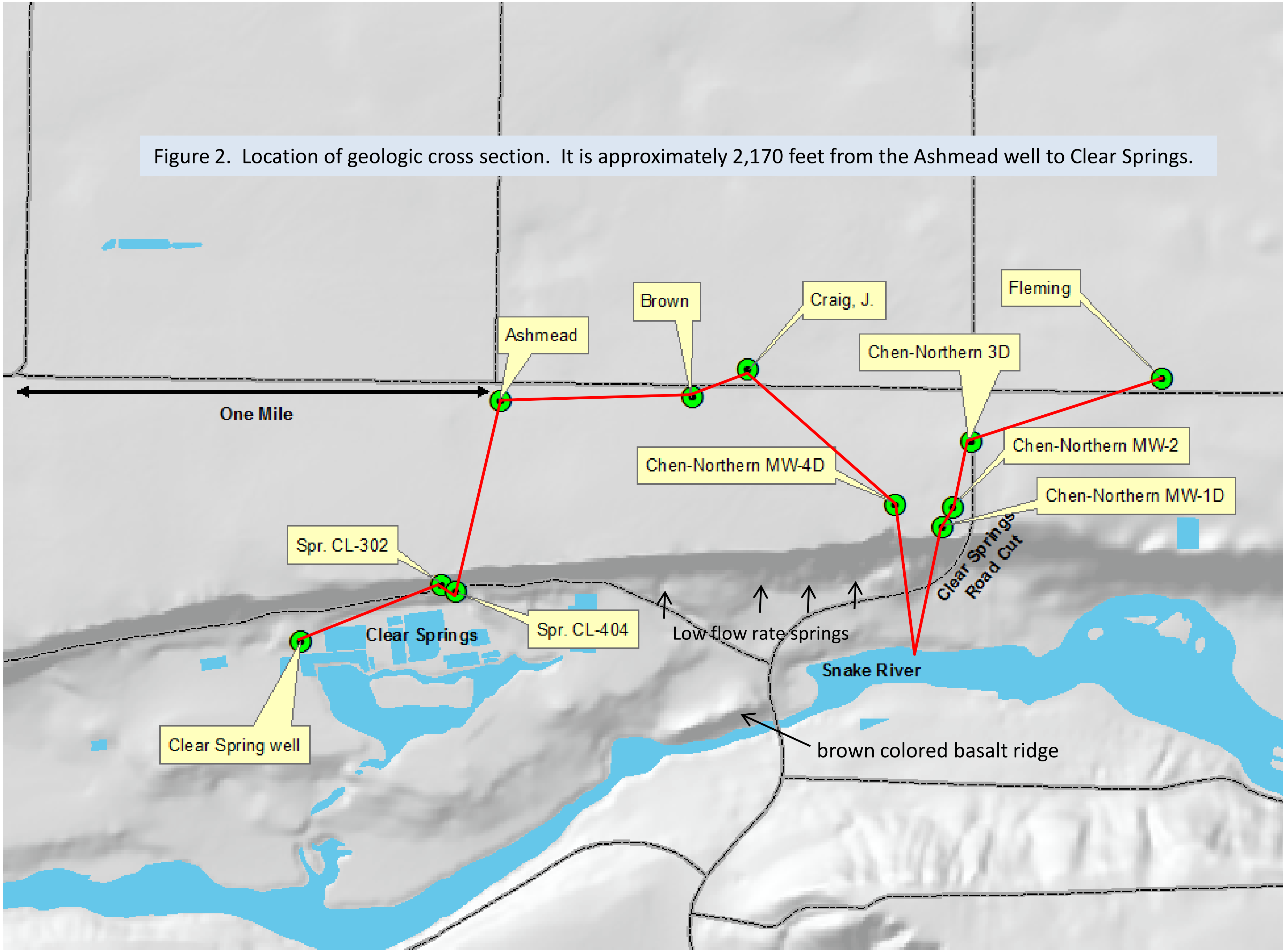
Figure 2. Location of geologic cross section. It is approximately 2,170 feet from the Ashmead well to Clear Springs.
One Mile
Ashmead
Brown
Craig, J.
Fleming
Chen-Northern 3D
Chen-Northern MW-2
Chen-Northern MW-4D
Chen-Northern MW-1D
Clear Springs Road Cut
Spr. CL-302
Spr. CL-404
Clear Springs
Low flow rate springs
Snake River
Clear Spring well
brown colored basalt ridge

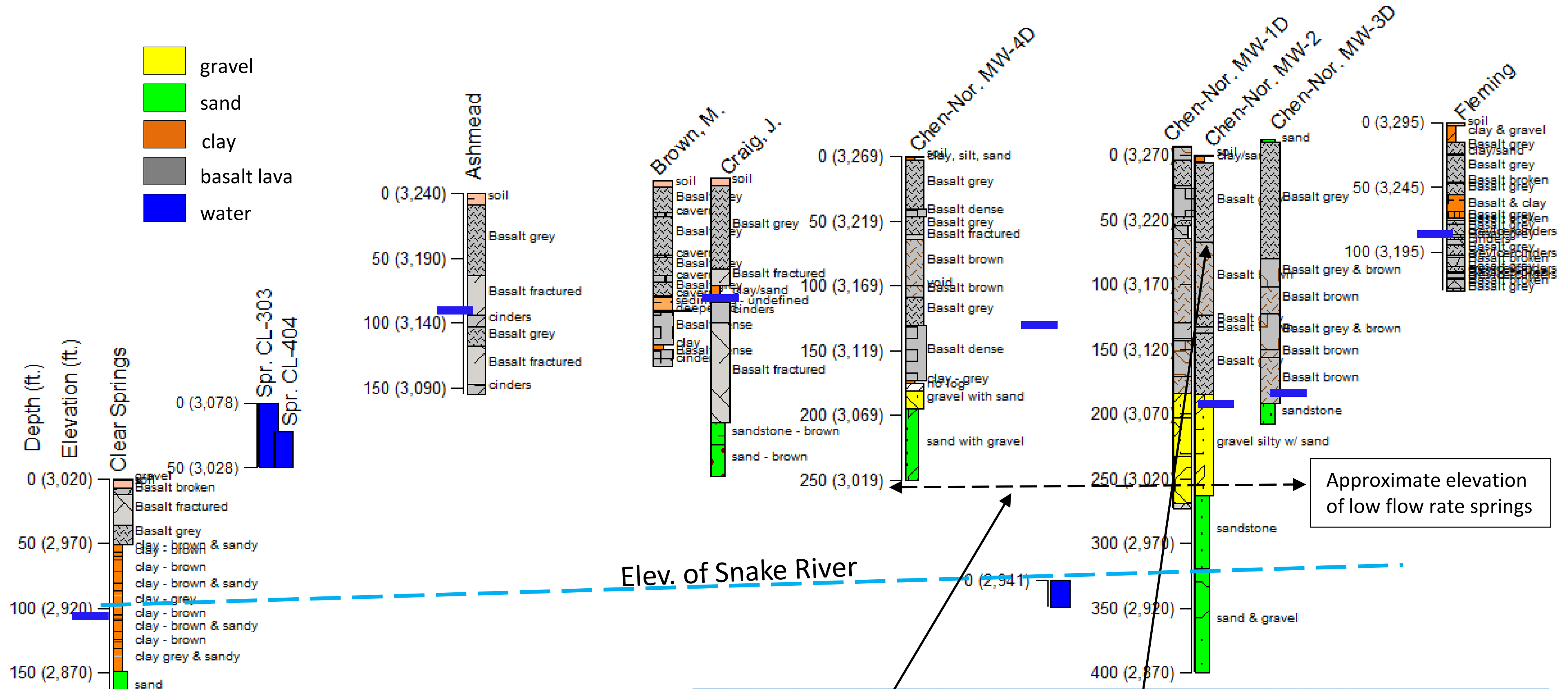

Figure 3. Geologic cross section showing basalt rock types with grey colored patterns, clay sediments as orange patterns, sand sediments as green patterns, gravel sediments as yellow patterns. Horizontal and vertical units are in feet and one mile between the Ashmead well and MW-3D well.

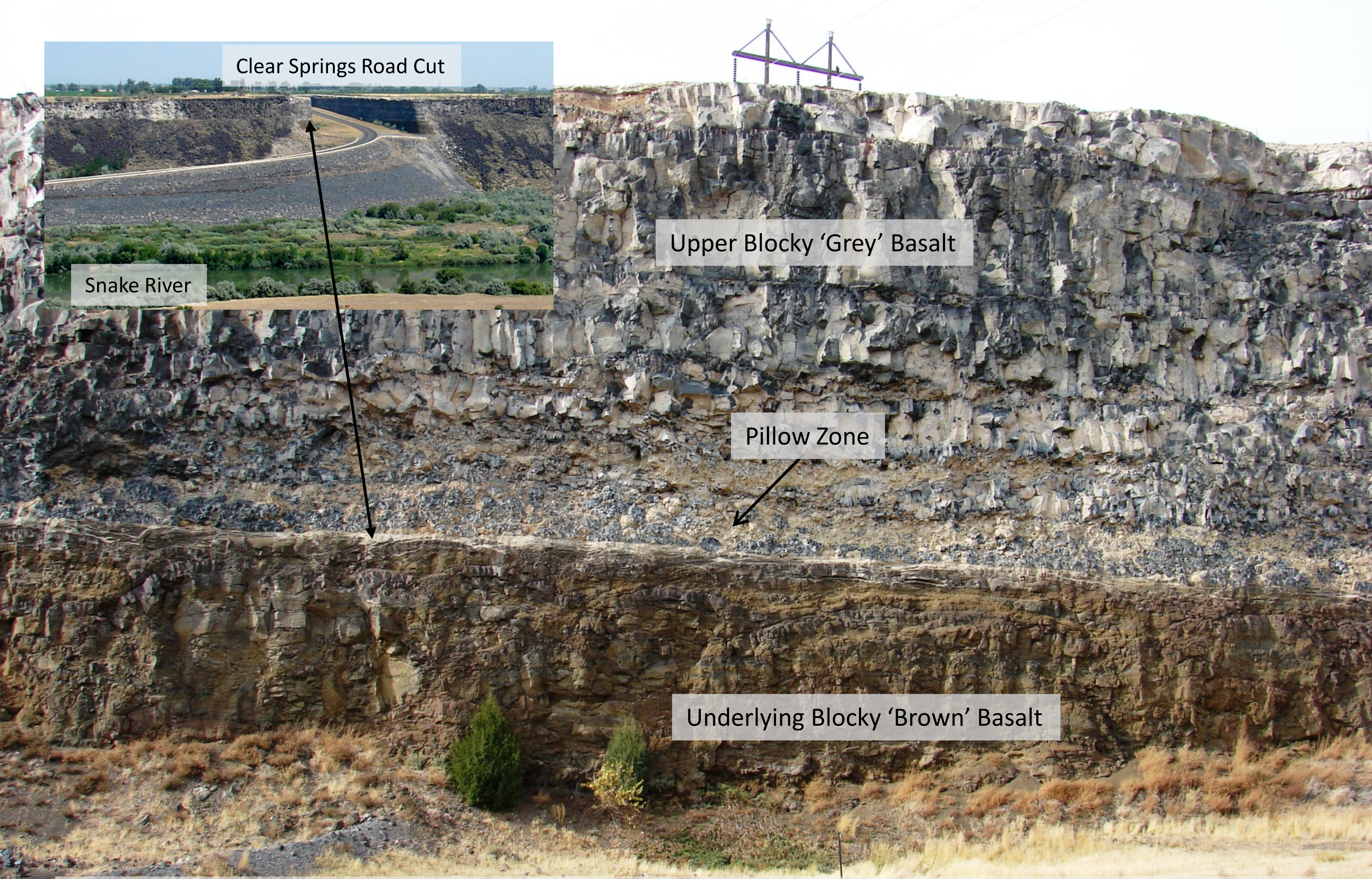

Figure 4. Clear Springs road cut showing quaternary age “grey” basalt overlying Tertiary age “brown” basalt with a pillow and sediment zone in between. There is a northerly dip to the exposed contact which correlates to a northerly dip from well geologic logs. Characteristics of the contact dip are forthcoming in a subsequent tracing report.

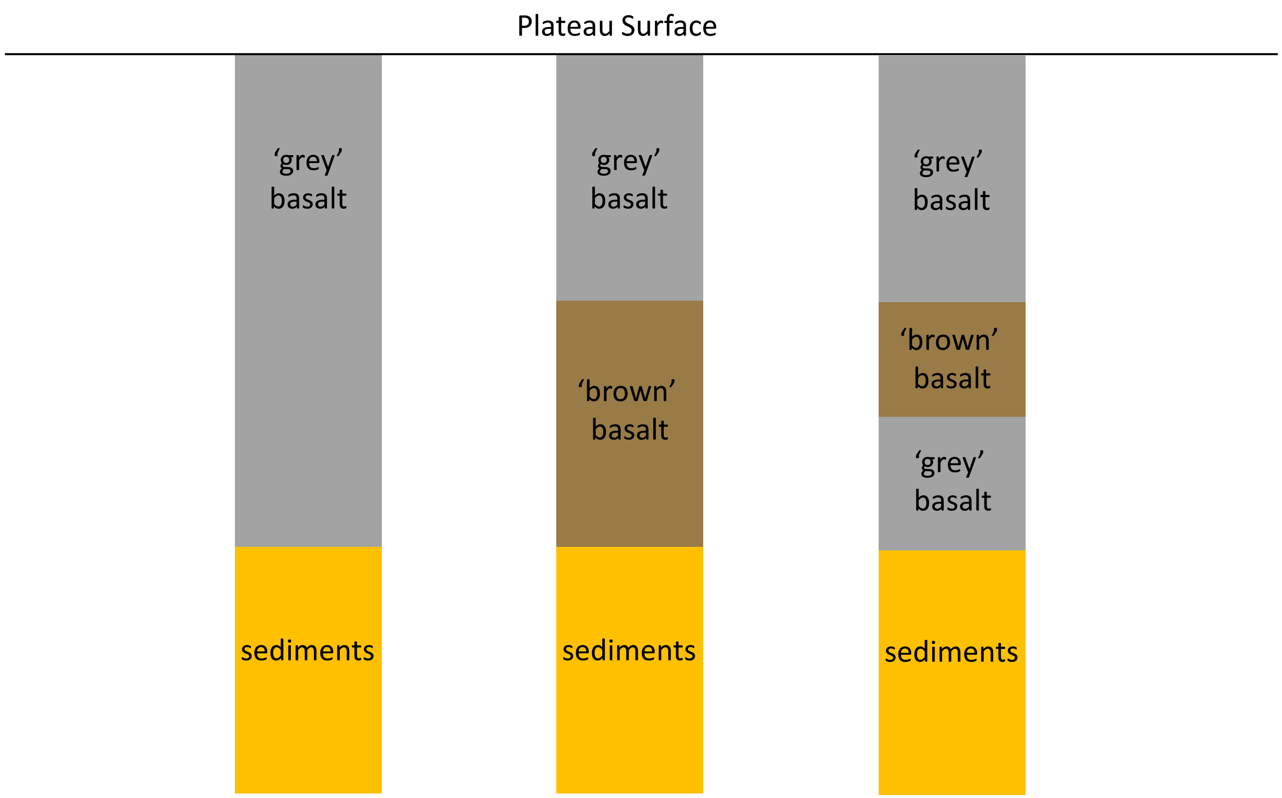

Figure 5. Three possible megascale stratagraphic models of the area near Clear Springs. The left model shows where the 'brown' basalt may be missing due to erosion of a paleo canyon and subsequent filling with more recent 'grey' colored basalts of Quaternary age. The middle column represents essentially the gross geology near the Clear Springs road cut where erosion has not removed the Tertiary age 'brown' basalt (based on road cut outcrop and MW-3D). The right column is based Chen-Northern monitor well 2 where 'grey' basalt underlies the brown basalt then sediments down to 400 foot depth or 70 feet below the river elevation .

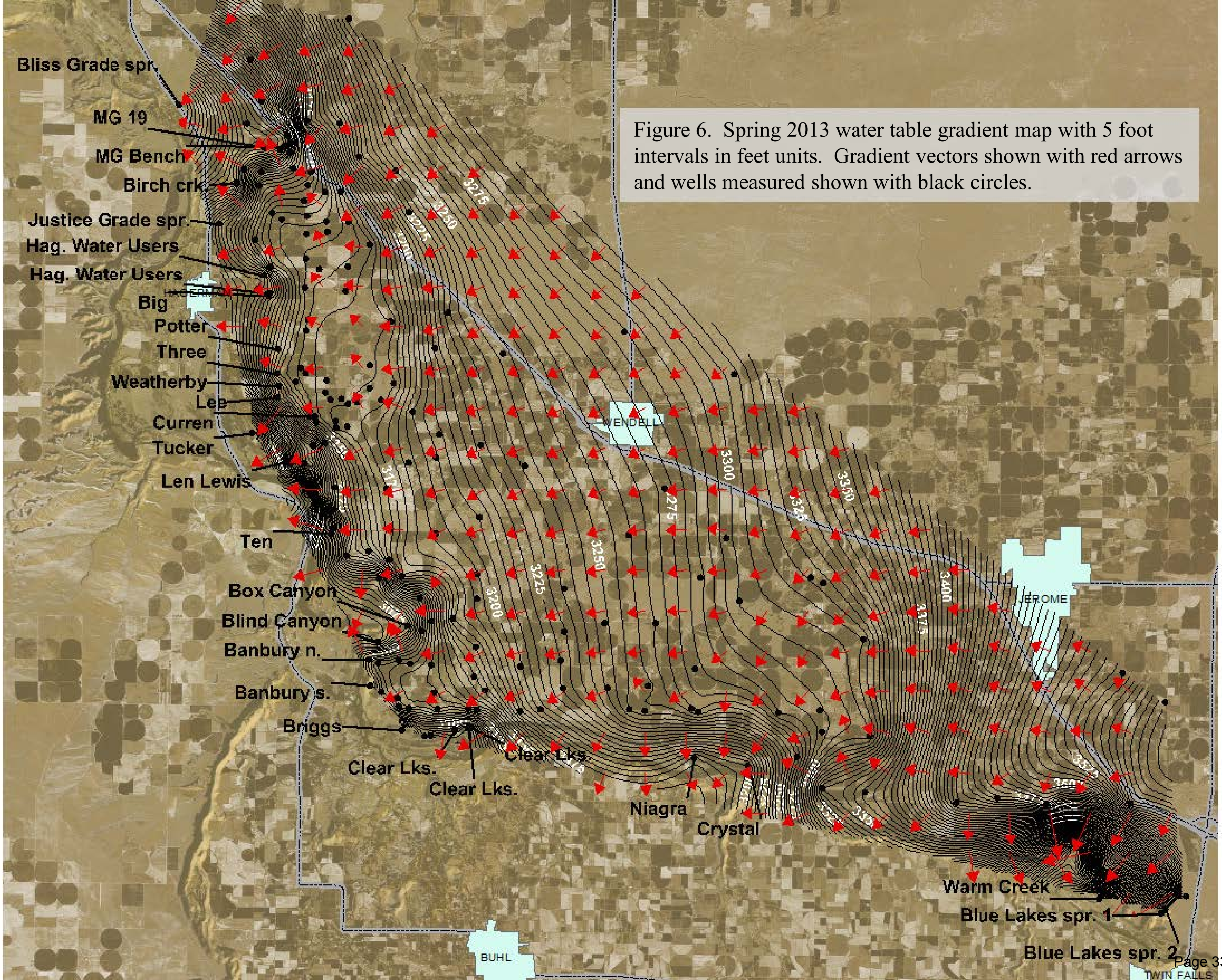

Figure 6. Spring 2013 water table gradient map with 5 foot intervals in feet units. Gradient vectors shown with red arrows and wells measured shown with black circles.

Figure 7. 3-D water table map showing 5 foot contour intervals in feet units. Arrows represent gradient direction and elevation legend is in feet units.

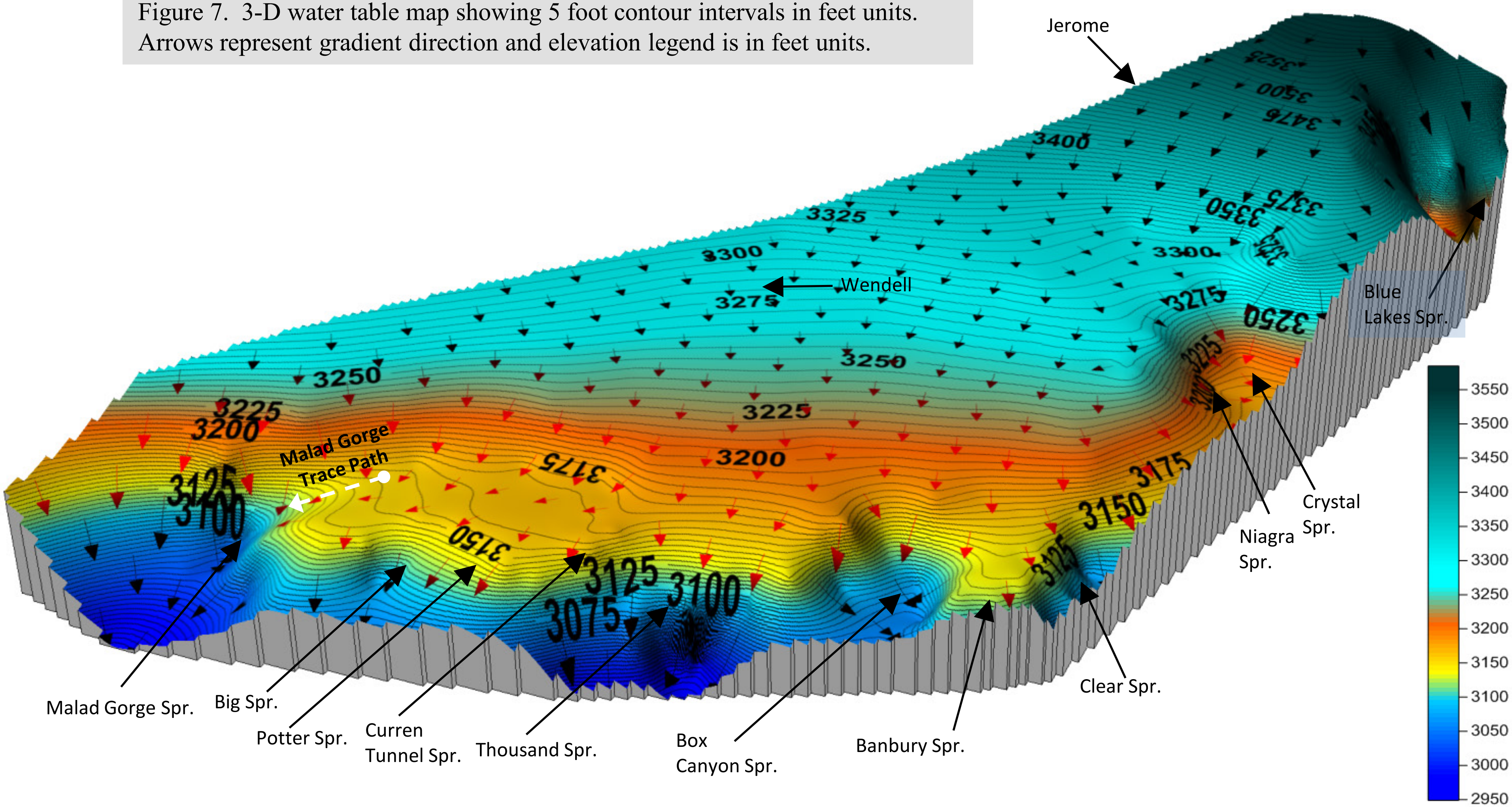

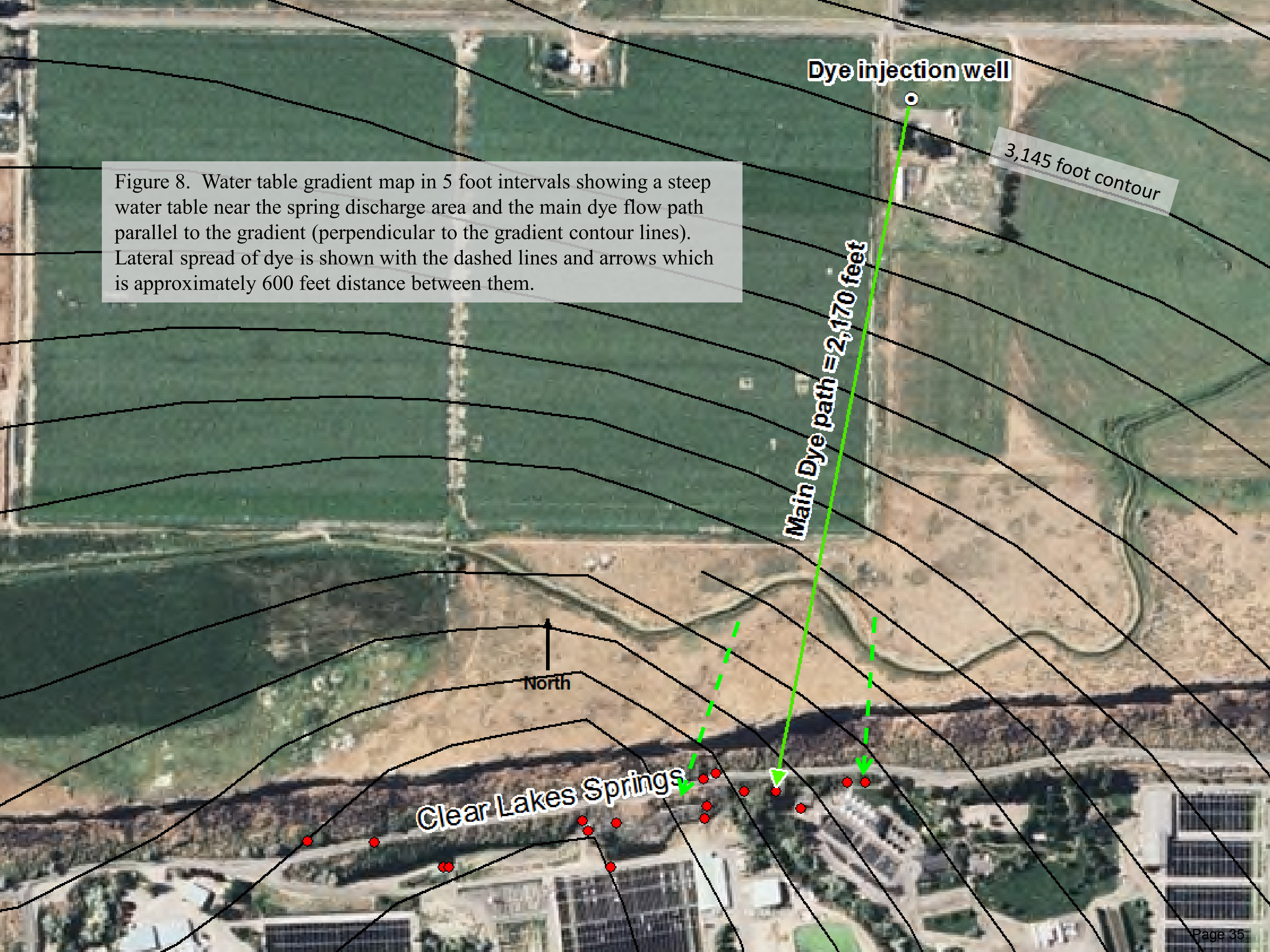

Figure 8. Water table gradient map in 5 foot intervals showing a steep water table near the spring discharge area and the main dye flow path parallel to the gradient (perpendicular to the gradient contour lines). Lateral spread of dye is shown with the dashed lines and arrows which is approximately 600 feet distance between them.

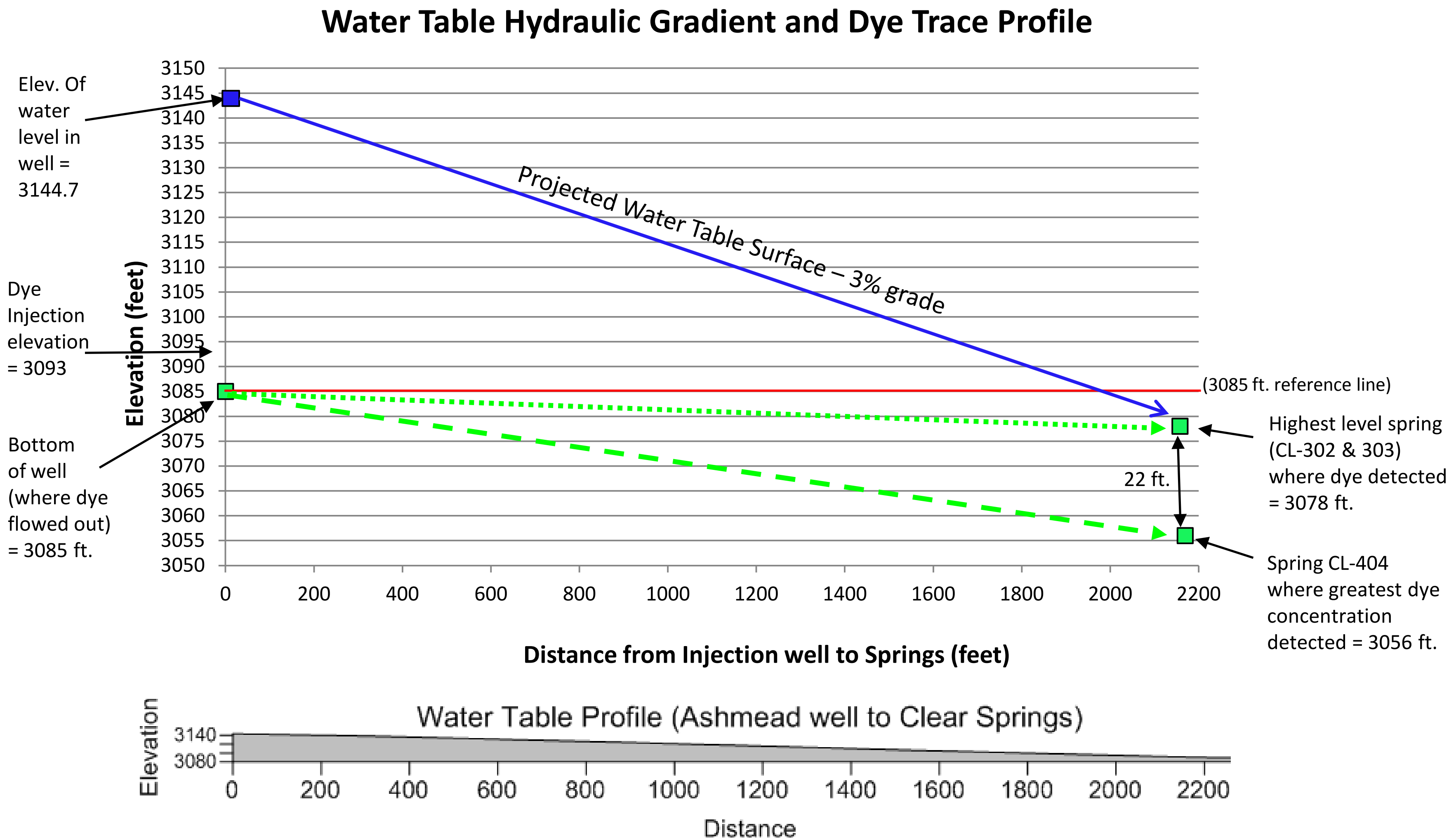

Figure 9. Water table gradient and dye path profiles from the Ashmead well to the spring area (2,170 ft. distance). The blue line represents the water table surface gradient from the well to the highest visible spring water emergence at site CL-303 for a vertical difference of 67 feet. The green square symbols and dashed line represent the level of dye exiting out of the well and spring sample site CL-404 where most of the dye emerged for a vertical difference of 29 feet. Note the main dye flow path (larger green dashed line) is flowing directly down gradient in the water table aquifer roughly parallel to the water table. There is approximately 22 vertical feet between CL-302 and CL-404 suggesting a vertical dispersivity in the aquifer between these spring sites. The lower profile displays the hydraulic gradient with no vertical exaggeration.

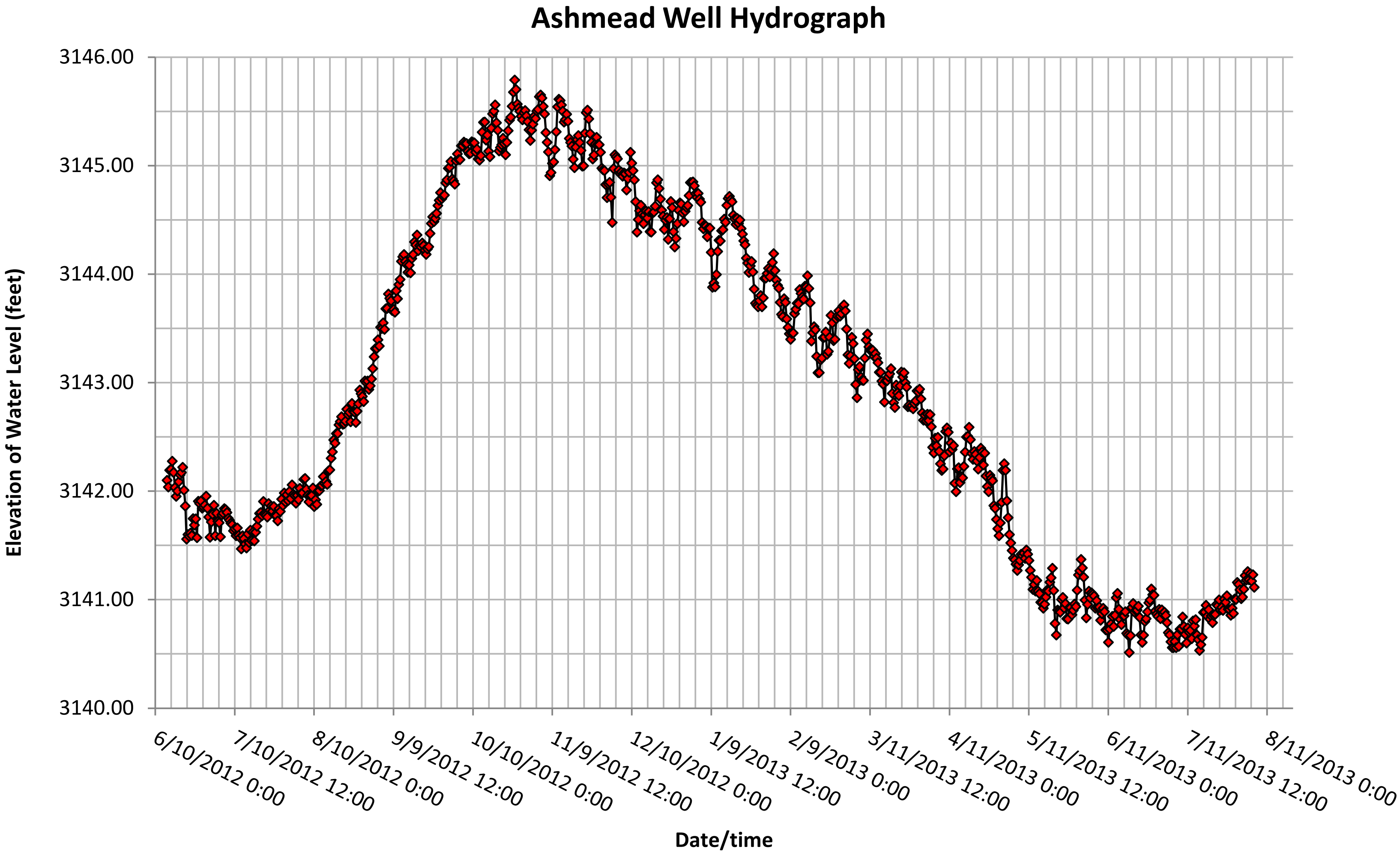

Figure 10. Water level hydrograph for the Ashmead well with a measurement frequency of every 12 hours.

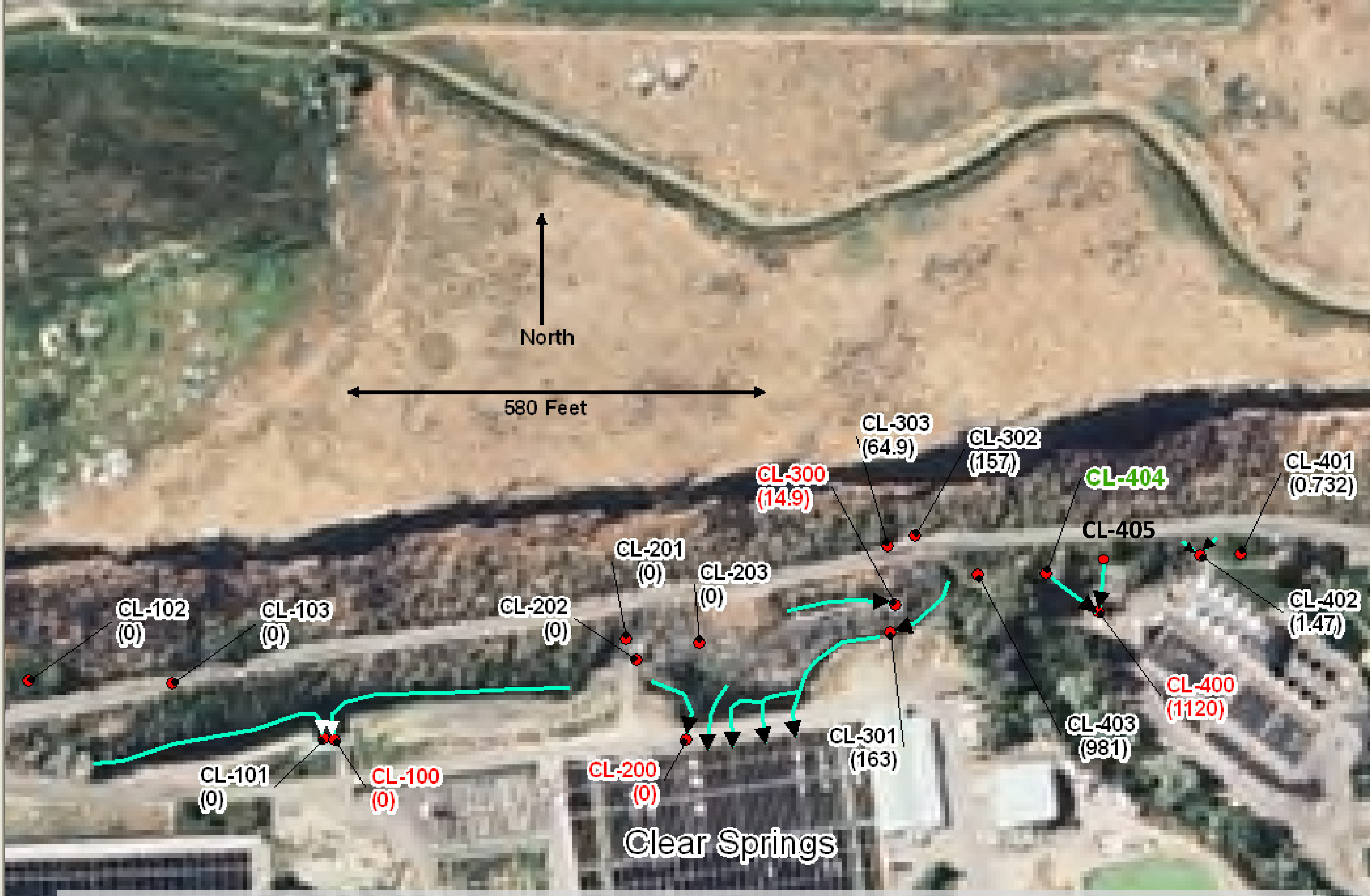

Figure 11. Detail map of the spring sample sites shown as red circles with leader lines to the site name and charcoal packet concentration noted in parenthesis as ppb FL from Trace #1. The light blue/green lines with arrow heads show general routing of spring water capture systems and basin flow. Site CL-404 had the highest dye concentration from water samples but a packet was not placed this spring.

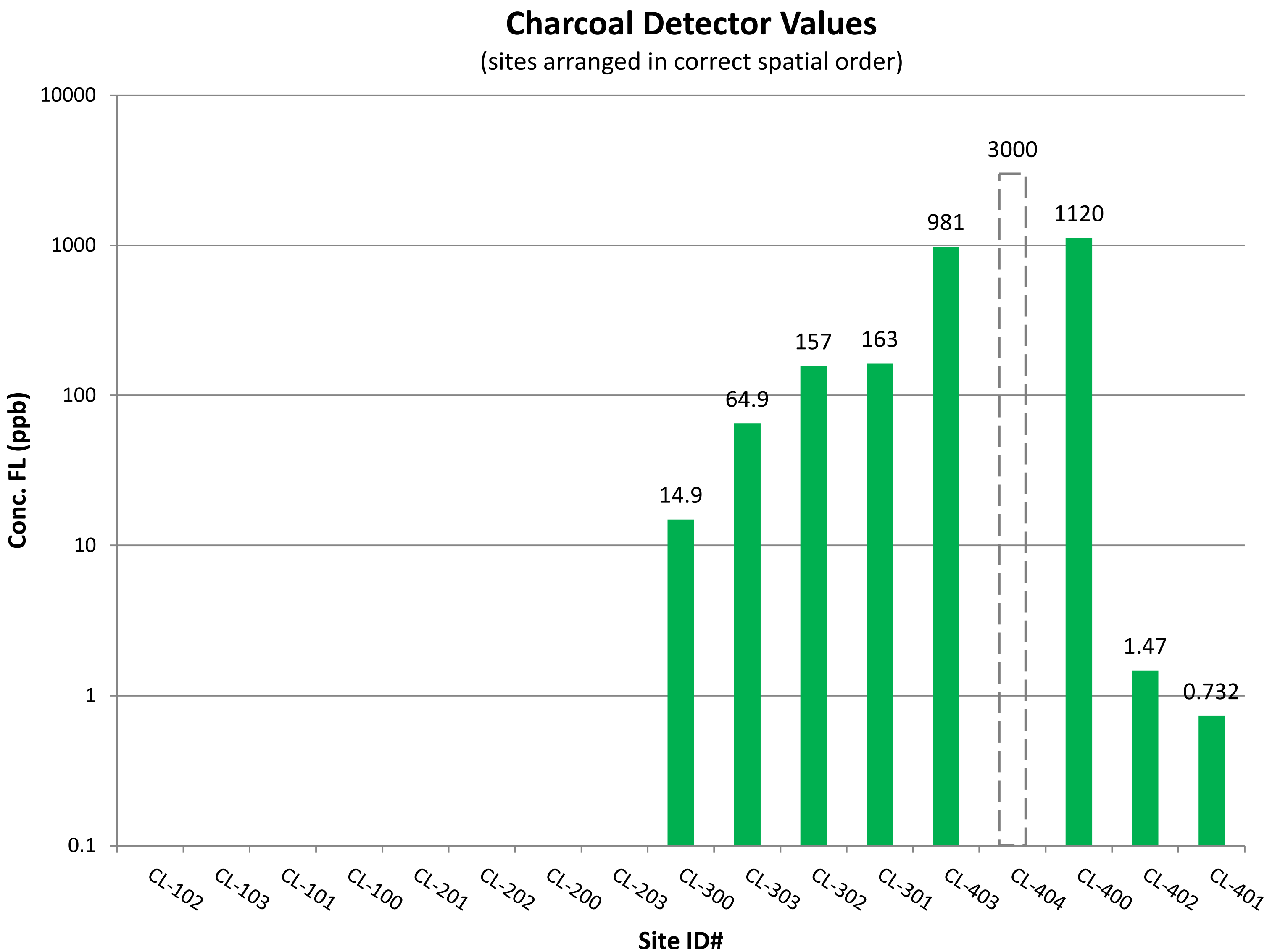

Figure 12. Analysis results for charcoal packet detectors in ppb units showing a typical rough bell shaped curve pattern to the horizontal spring discharge area. Site CL-404 is inferred and projected in the graph because no detector was deployed at this spring.

Site ID	Easting (meters)	Northing (meters)	GPS Elev. (feet)	1st Trace Packet Conc (ppb)	Comment
CL-100	2436333	1275166	3033	0	cl-100 weir instrument
CL-101	2436328	1275166	3036	0	cl-101 packet hanging off bridge
CL-102	2436201	1275191	3063	0	cl-102 packet in cave spr.
CL-103	2436263	1275190	3083	0	cl-103 packet on rock at pipe in
CL-200	2436484	1275166	3041	0	cl-200 head ditch instrument
CL-201	2436458	1275209	2918	0	cl-201 packet in culvert
CL-202	2436463	1275200	3032	0	cl-202 packet in stream bottom
CL-203	2436490	1275207	3031	0	cl-203 packet in spring
CL-300	2436574	1275223	3043	14.9	cl-300 cement box instrument
CL-301	2436572	1275211	3035	163	cl-301 pipeline walkway packet
CL-302	2436583	1275241	3078	157	cl-302 drink spring packet
CL-303	2436571	1275249	3078	64.9	cl-303 pack on rock in spr
CL-400	2436662	1275221	3055	1120	cl-400 collection box instrument
CL-401	2436723	1275246	3061	0.732	cl-401 impacted spr
CL-402	2436705	1275245	3058	1.47	cl-402 cement box
CL-403	2436610	1275236	3043	981	cl-403 water fall
CL-404	2436639	1275237	3056	no packet deployed	cl-404 spr. collection metal grate

Table 1. List of spring sample sites with dye concentrations from packets for Trace #1. Sites CL-100, CL-200, CL-300, CL-400 are locations with Fluorometers but site CL-404 had the highest concentration of dye based on water samples. Site CL-400 charcoal packet had the highest packet concentration but no packet was deployed at CL-404. Analysis was performed by a private lab at Ozark Underground Labs.

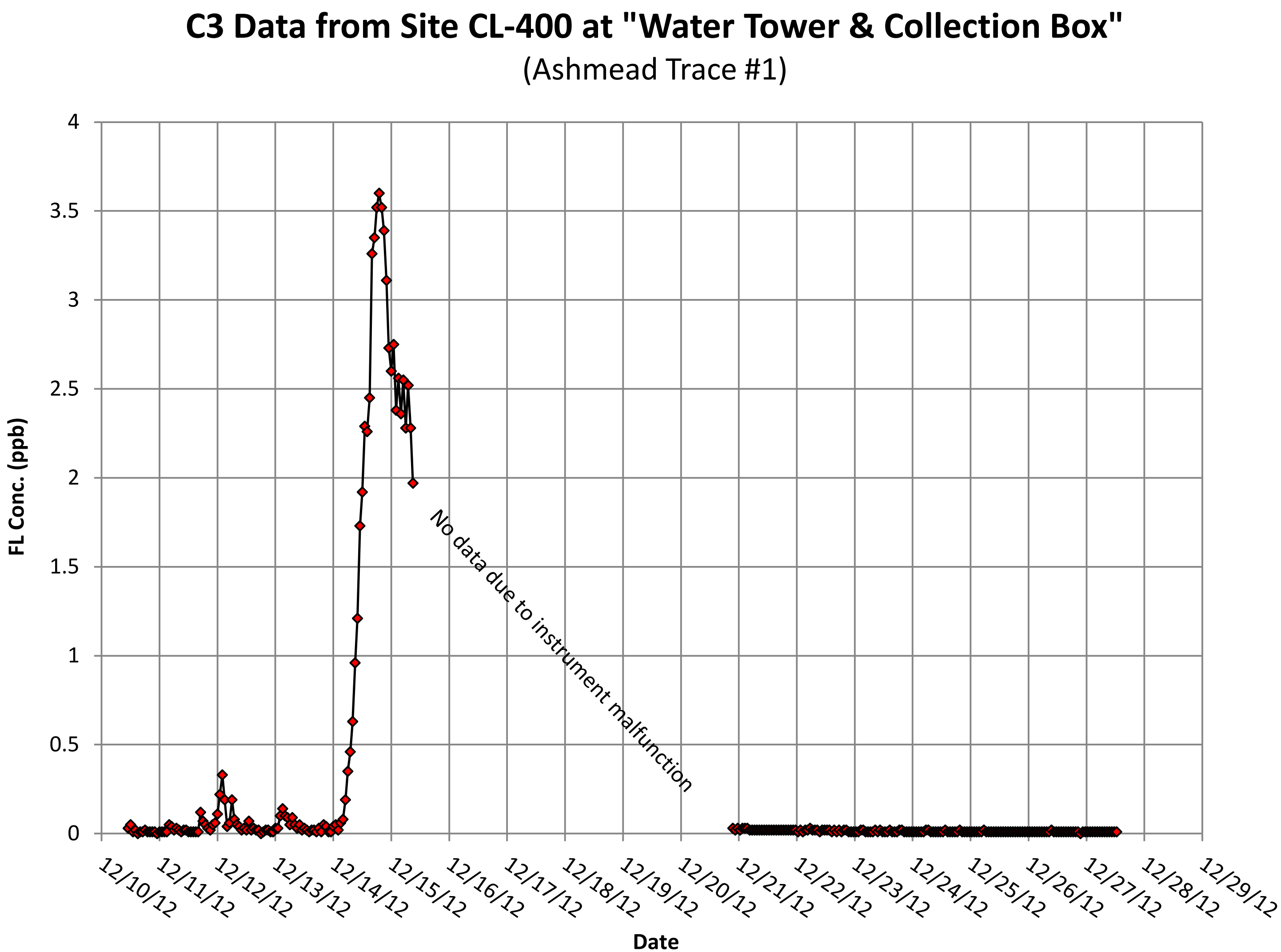

Figure 13. C3 instrument data from site CL-400 showing a dye breakthrough curve with hourly frequency showing a clear arrival of dye and peak. Most of the recession limb data was lost due to instrument malfunction.

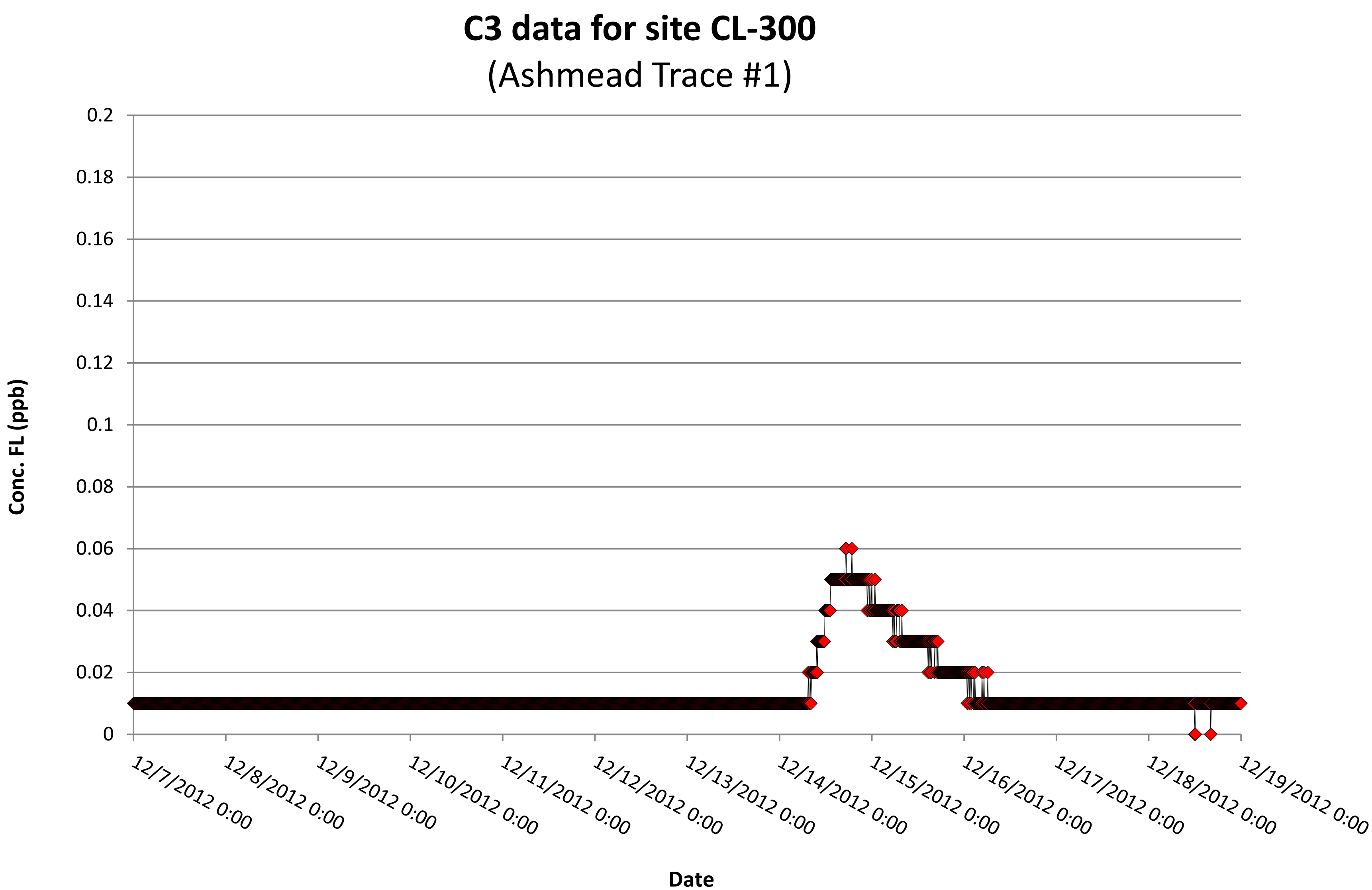

Figure 14. Dye breakthrough curve for site CL-300 with a peak of approximately 0.05 ppb. Located in "Hatch House" collection box and data is 10 minute intervals.

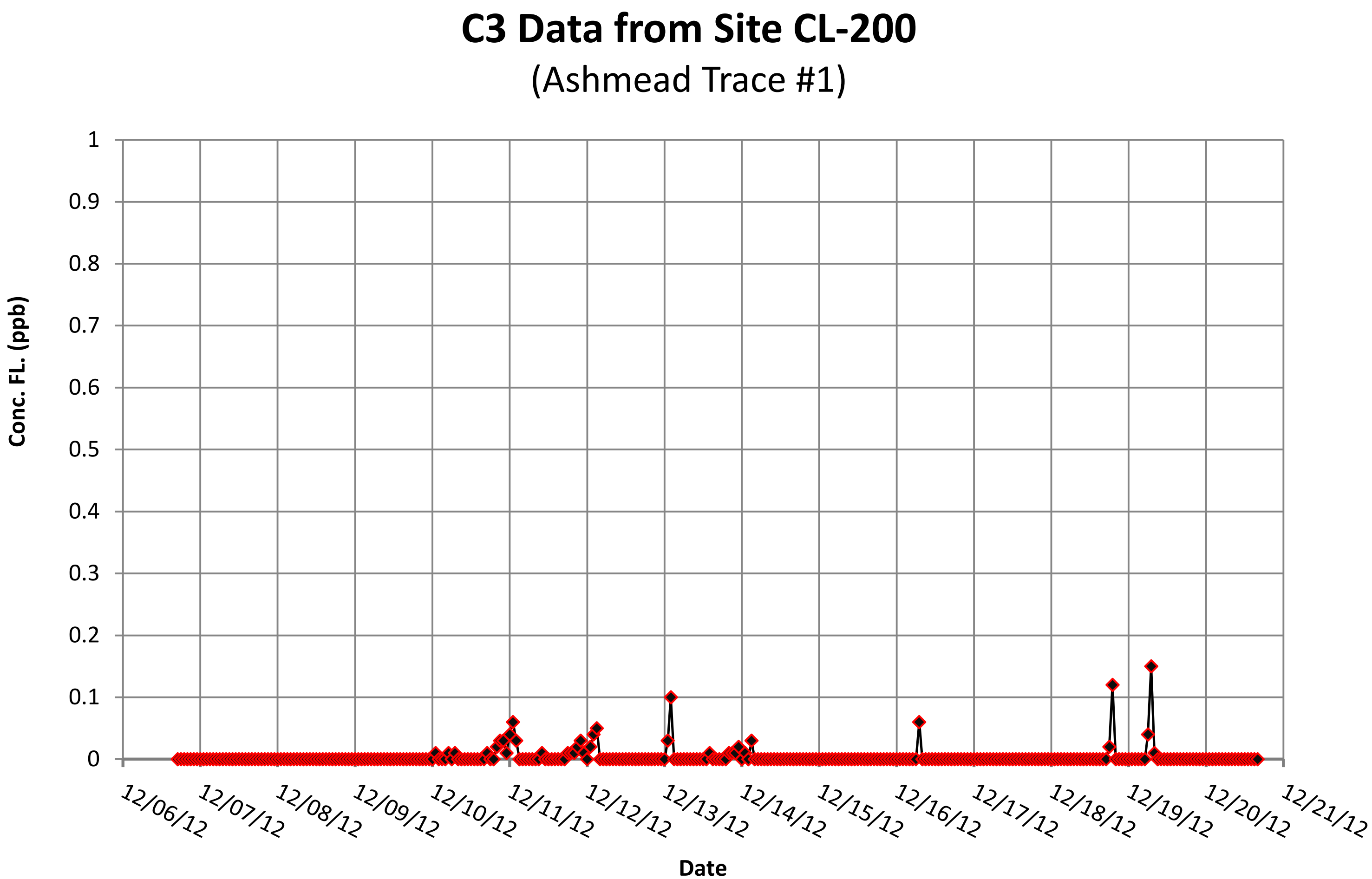

Figure 15. Results for C3 instrument from site CL-200 showing no discernible detection of dye but some noise.

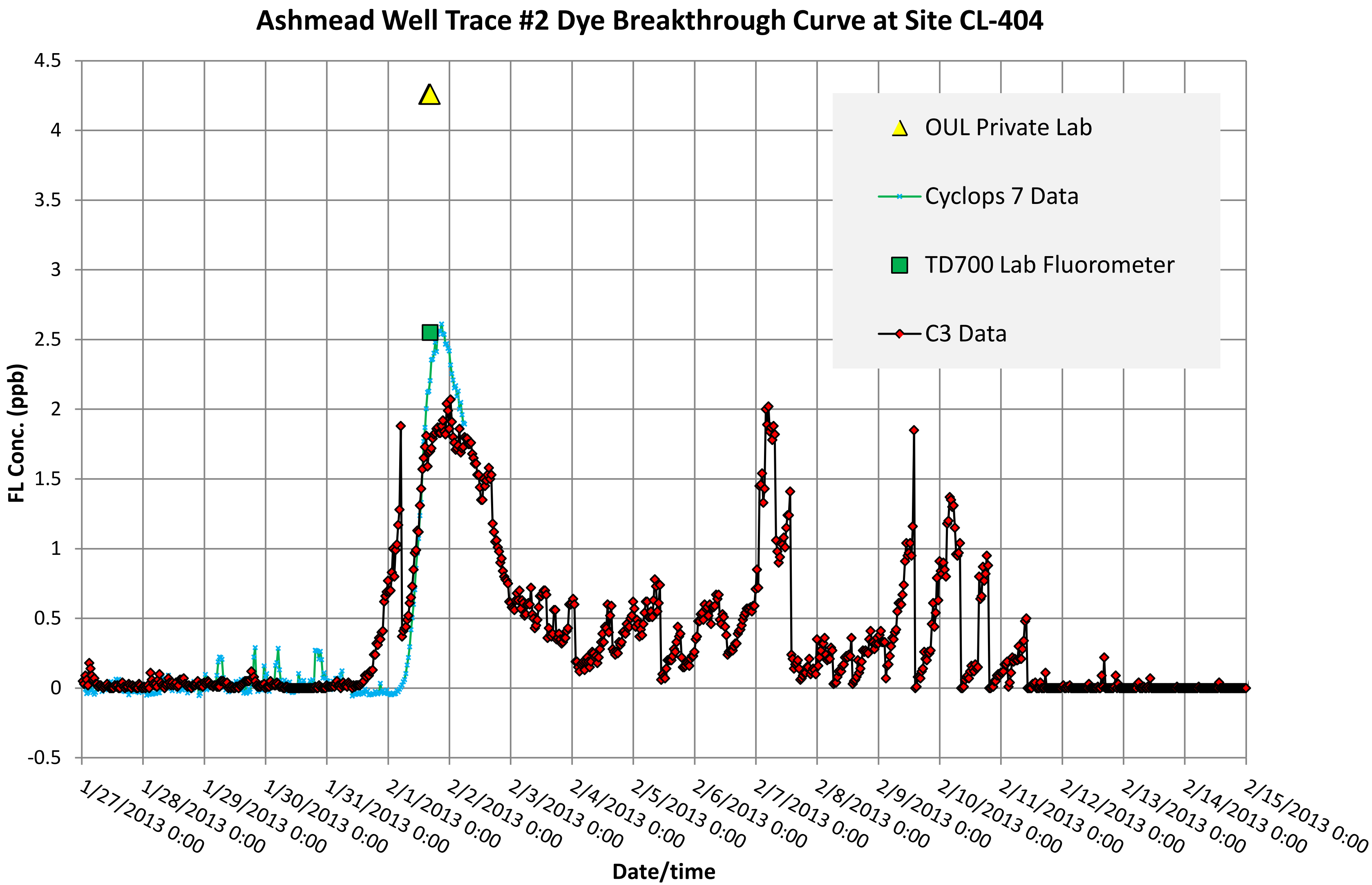

Figure 16. Graph showing the Cyclops instrument data as blue line/symbols, C3 instrument data as red symbols, TD700 lab fluorometer as green square and OUL Labs results with a yellow triangle. These data sets were integrated to form the breakthrough curve in Figure 17.

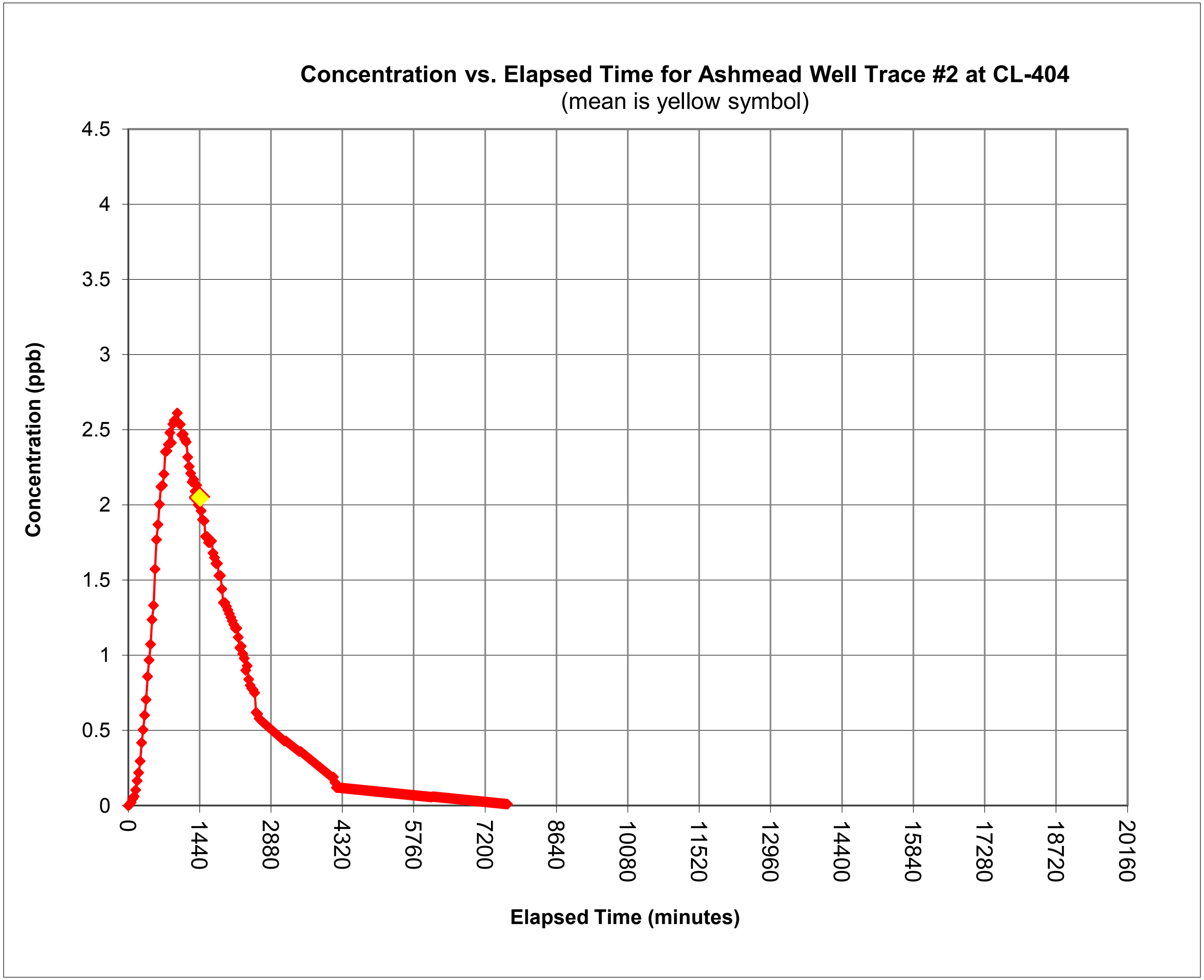

Figure 17. Integrated dye breakthrough curve for site CL-404 using data from both the C3 instrument and Cyclops 7 instrument (Figure 16) that were deployed together in the same spring.

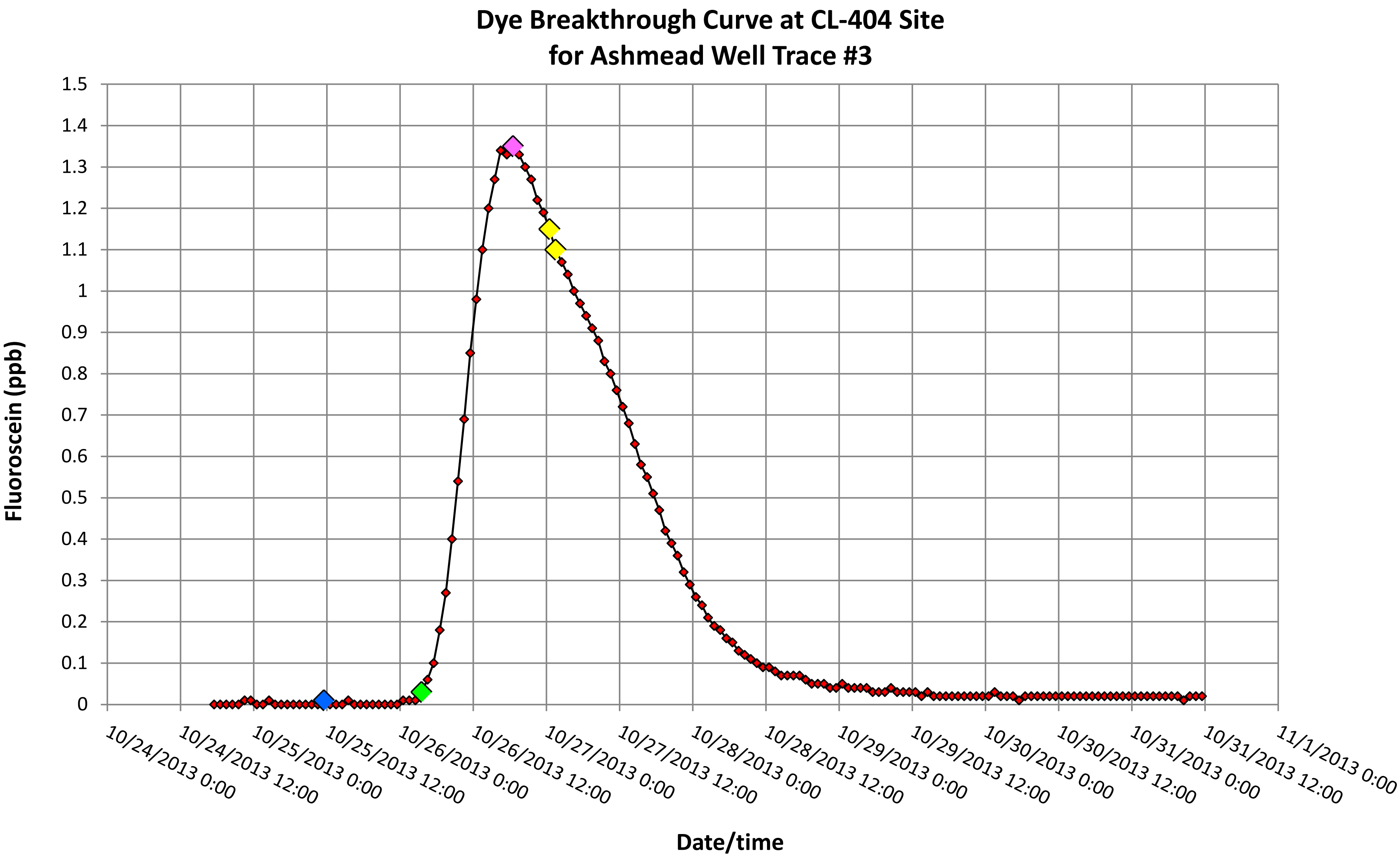

Figure 18. Year 2013 trace #3 dye breakthrough curve for site CL-404 using data from a C3 instrument. Note the clear single peak, steep rising limb, lower angle recession limb, and the mean. Injection occurred at the time shown with the blue triangle, first dye arrival with a green triangle, peak with pink triangle, and the mean was calculated to be between the two yellow triangle data points.

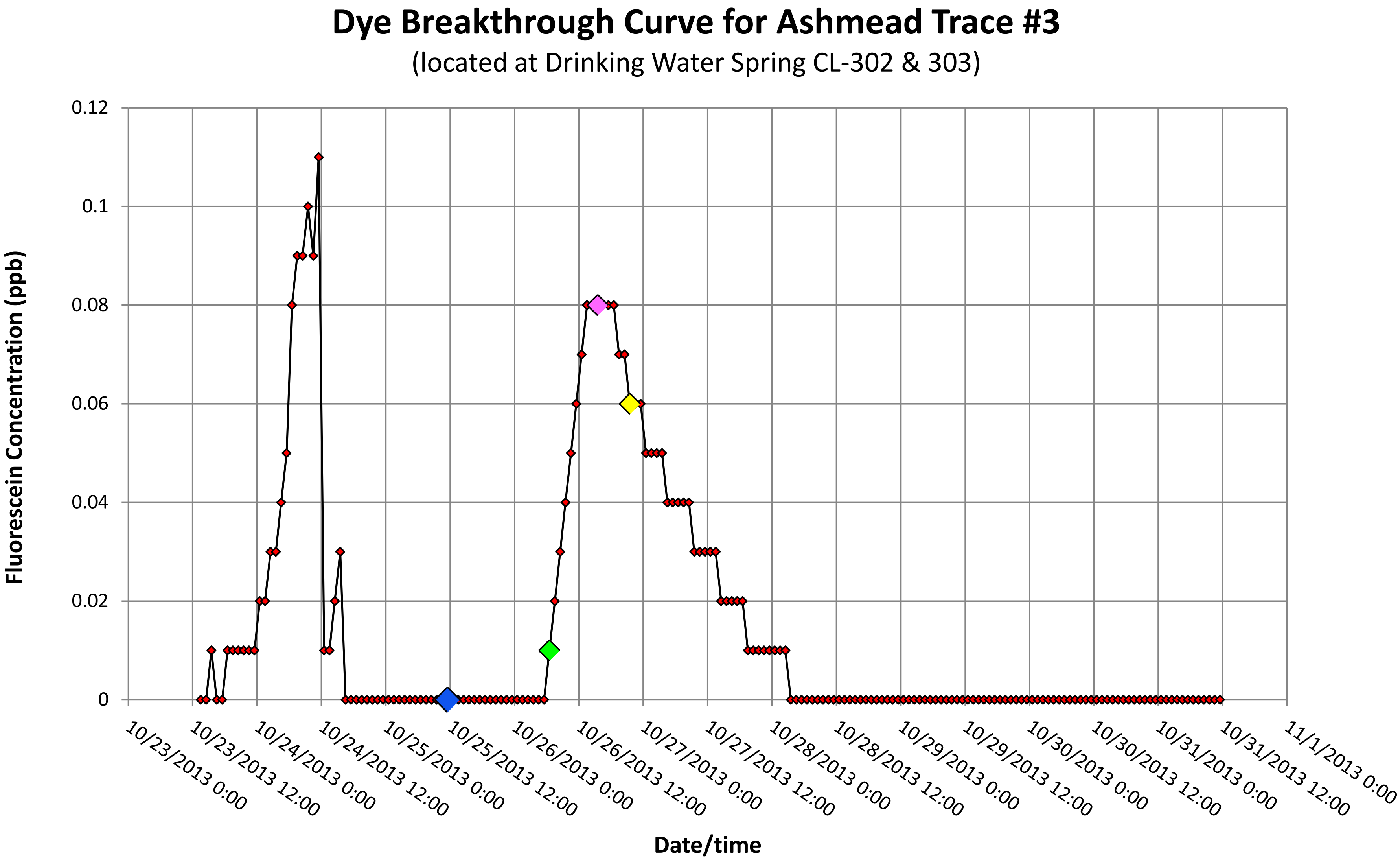

Figure 19. Year 2013 trace #3 dye breakthrough curve for site CL-302&303 combined spring water using data from a C3 instrument. Injection occurred at the time shown with the blue diamond, first dye arrival with a green diamond, peak with pink diamond, and the mean was calculated to be at the yellow diamond data point. The peak before injection on the 24th is pre-injection background noise. Note the clear single peak, steep rising limb, lower angle recession limb, and the mean.

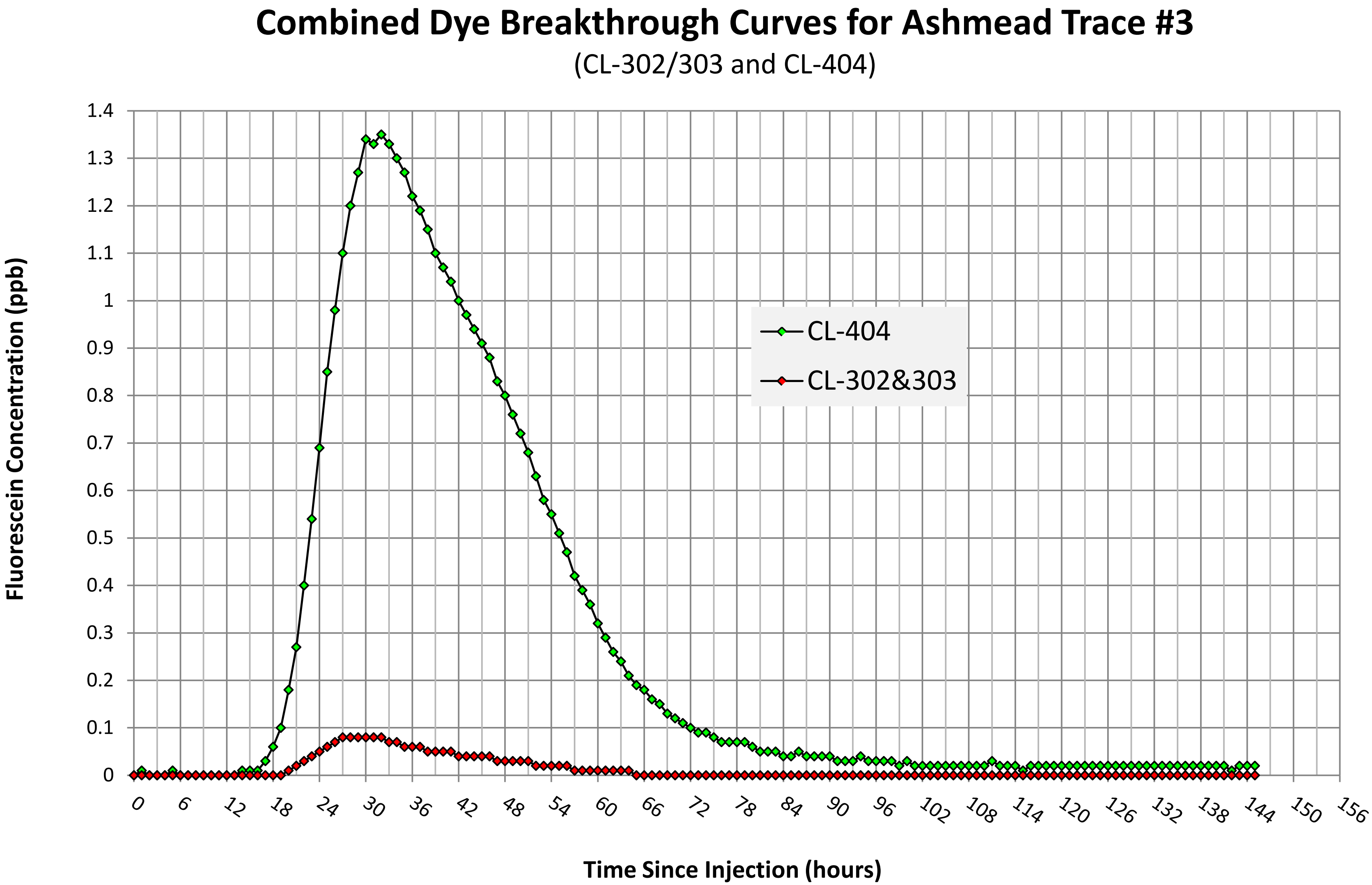

Figure 20. Combined breakthrough curves for year 2013 trace #3 at the Ashmead well with data plotted since time zero since injection (t_0). Data points are at 1 hour intervals. Note the first arrival is delayed by approximately 3 hours for the CL-302&303 site but the peaks are very similar in timing. The first arrival of dye at CL-302&303 may have been present at the same time as site CL-404 but below detection limits of the instrument.

Hydrogeologic Model of Canyon Wall and Talus Slope

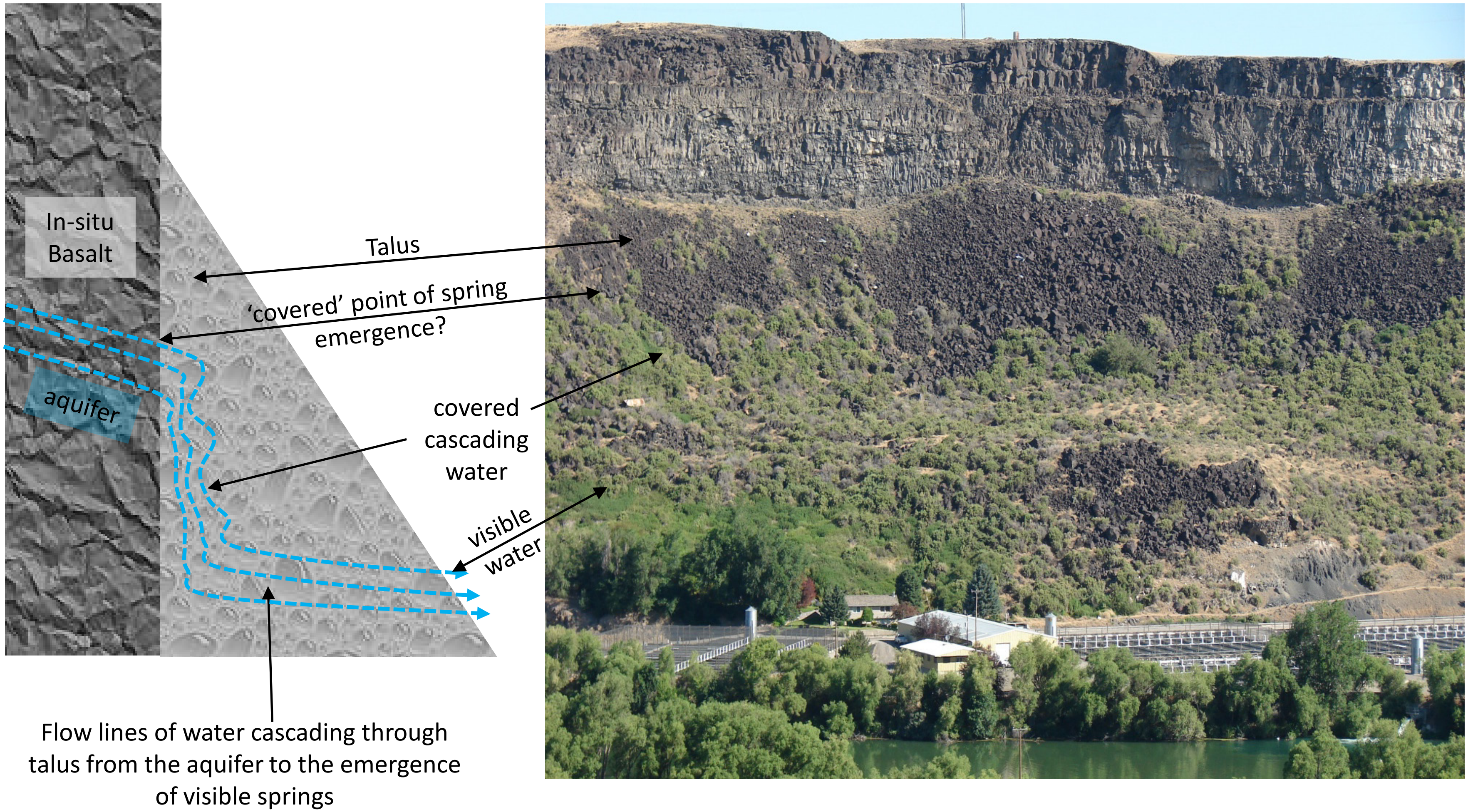

Figure 21. A hydrogeologic model showing how aquifer discharge water may flow through the talus slope at spring areas. Photo is of Crystal Spring area.

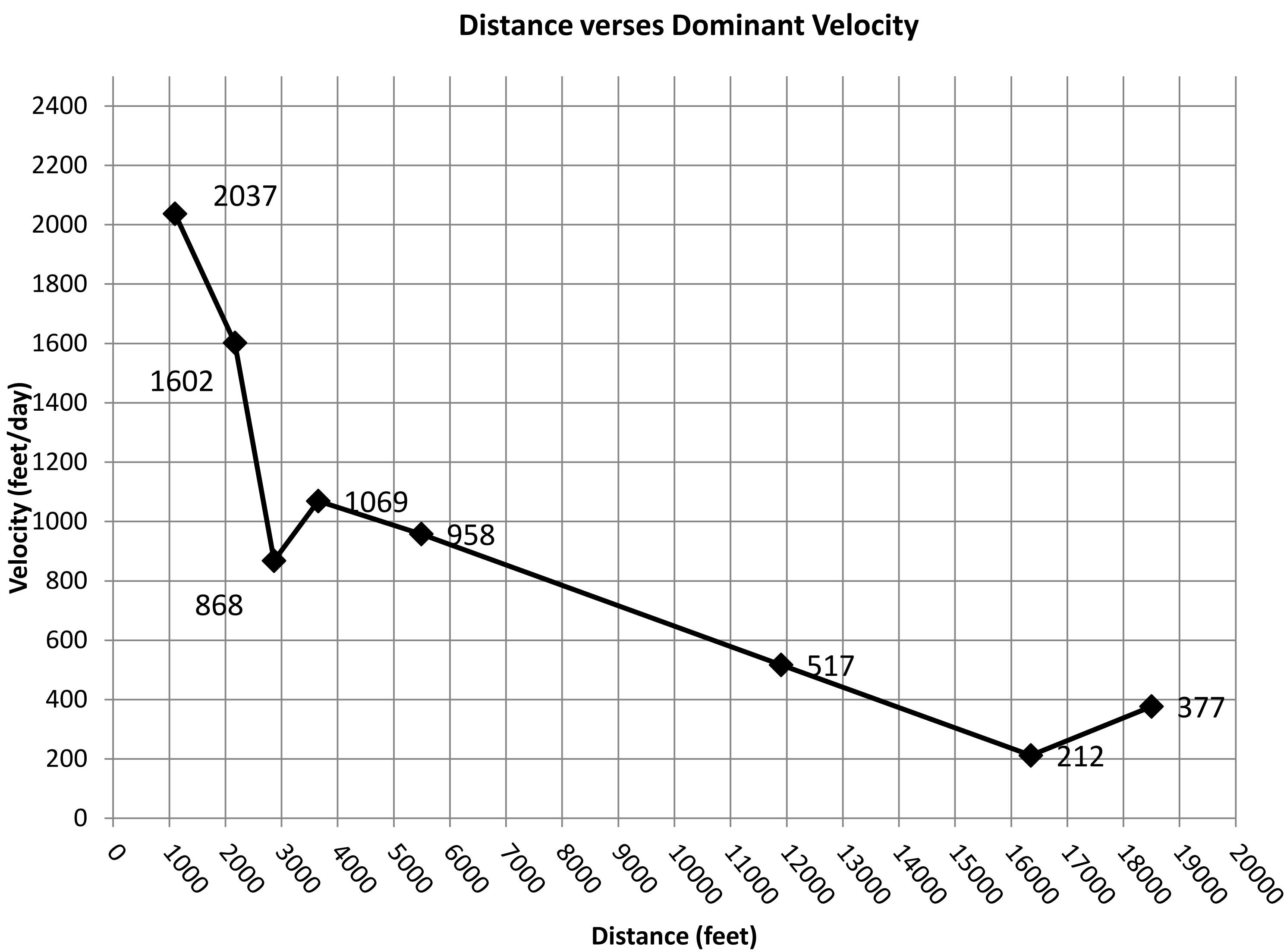

Figure 22. Chart of tracer test distance verses dominant velocity (based on breakthrough curve peak) showing how as distance from spring discharge areas increases velocity decreases.

Date	Time	Trace Name	Elev. of well TOC MP (RTK GPS'd in feet)	Depth to Water (feet below TOC MP)	Elev. Of Water Table (feet a.m.s.l.)	Depth of Dye Injection (below T.O.C.)	Straight Line Distance (feet)	Dye (type & mass)	Volume of dye mixture released (gallons)	Time to First Dye Arrival (hours)	Max GW Velocity (ft./day)	Time to Mean Concentration (hours)	Ave. GW Velocity (ft./day)	Time to Peak Concentration (hours)	Dominant Flow Velocity (ft./day)	Measured Transverse Dispersivity (feet)	Measured Longitudinal Dispersivity (feet)	Interpolated Longitudinal Dispersivity (feet)	Approx. Time of Passage (days)	Peak Water Conc. (ppb)	Peak Charcoal Packet Conc. (ppb)	Elev. of Peak Conc. Sample Site	Elev. of highest spr. Water[b]	Effective Porosity (estimate) 'Pe'	Reynolds number 10 met at Passage Way Diameter (inches) (or larger)	Gradient (at highest spr.)	Gradient (Increase Spr. Elv. by 25 ft.)[b]	Hydraulic Conductivity K=(Pe*Vave)/I Pe=0.20	Hydraulic Conductivity (higher elev. spr.) K=(Pe*Vave)/I Pe=0.20
April 7, 2009	5:10 PM	Park picnic	3275.46	n.a.	n.a.	215	1,100	1 lb. FL (75% conc.)	3	n.a.	n.a.	n.a.	n.a.	n.a.	n.a.	450 (MG6-10.5)	n.a.	n.a.	n.a.	n.a.	1310 @ MG-7	3031	3046	0.2	n.a.	n.a.	n.a.	n.a.	n.a.
June 23, 2009	3:31 PM	Park picnic 1	3275.46	191.06	3084.4	210	1,100	0.21 lb. RWT (100% conc.)	1 (2.5% conc.)	5	5,280	n.a.	n.a.	12.5 & 35	1^{st} peak = 2,112 2nd peak = 754	n.a.	n.a.	n.a.	4.2 (estimated)	0.37 @ MG-7	n.a.	3031	3046	0.2	0.73	0.035	0.0258	n.a.	n.a.
June 29, 2009	1:52 PM	Park picnic 2	3275.46	n.a.	n.a.	210	1,100	0.21 lb. RWT (100% conc.)	1 (2.5% conc.)	4.5	5,867	30.3	871	13.5 & 34	1^{st} peak = 1,955 2nd peak = 776	n.a.	n.a.	n.a.	4.2 (estimated)	0.43 @ MG-7	n.a.	3031	3046	0.2	0.73	0.035	0.0258	4977	6752
Sept. 22, 2009	2:30 PM	Park picnic 3	3275.46	190.28	3085.18	210	1,100	0.63 lb. RWT (100% conc.)	3 (2.5% conc.)	4.5	5,867	30.3[b]	871[b]	13 & 33.5	1^{st} peak = 1,955 2nd peak = 788	n.a.	n.a.	n.a.	4.2	0.91 @ MG-7	n.a.	3031	3046	0.2	0.73	0.036	0.0265	n.a.	n.a.
Oct. 20, 2009	12:30 PM	R. Riddle 1	3279.69	178.13	3101.56	205	2,865	3 lb. FL (75% conc.)	6	n.a.	n.a.	n.a.	n.a.	n.a.	n.a.	700 (MG2-7)	n.a.	n.a.	n.a.	n.a.	8160 @ MG-3	3029	3046	0.2	n.a.	0.019	0.0166	n.a.	n.a.
March 1, 2010	2:30 PM	R. Riddle 2	3279.69	177.95	3101.74	203	2,865	2 lb. RWT (100% conc.)	4	28	2,456	86	800	82	839	700 (MG1-6)	n.a.	n.a.	16	1.8 @ MG-3	388 @ MG-3	3029	3046	0.2	0.81	0.019	0.0167	8219	9596
April 19, 2010	10:45 AM	R. Hopper 1	3306.57	182.15	3124.42	192	5,490	4.84 lb. FL (75% conc.)	7.75	n.a.	n.a.	n.a.	n.a.	n.a.	n.a.	850 (MG1-5)	>2865	4177	n.a.	n.a.	1498 @ MG-2.5	3028	3046	0.2	n.a.	0.014	0.0130	n.a.	n.a.
May 21, 2010	1:00 PM	R. Hopper 2	3306.57	182.4	3124.17	192	5,490	5.01 lb. FL (75% conc.)	8	66	1,996	198	665	139	948	850 (MG1-5)	>2865	4177	17	1.10 @ MG-2.5	1640 @ MG-2.5	3028	3046	0.2	0.96	0.014	0.0130	9347	10267
Dec. 17, 2010	2:35 PM	Meyer 1	3334.55	180.78	3153.77	205	11,900	8 lb. FL (75% conc.)	15	260	1,098	626	456	528	541	1140 (MG7-13)	>6320	9185	40	0.37 @ Bench spr.	489 @ MG-4	3033	3046	0.2	n.a.	0.009	0.0080	10075	n.a.
March 25, 2011	3:00 PM	Meyer 2	3334.55	183.21	3151.34	205	11,900	14 lb. FL (75% conc.)	14	261	1,094	671	426	552	517	n.a.	>6320	9185	41	0.59 @ Bench spr.	744 @ MG-4	3033	3046	0.2	1.57	0.009	0.0078	9617	10853
June 7, 2011	11:30 AM	N. Riddle 1	3266.5	172.1	3094.4	171	2,660	0.46 lb. RWT (100% conc.)	0.25	n.a.	n.a.	n.a.	n.a.	n.a.	n.a.	300 (MG18-20)	n.a.	n.a.	n.a.	n.a.	76.75 @ MG-19	3026	3026	0.2	n.a.	0.026	0.0163	n.a.	n.a.
July 11, 2011	2:00 PM	R. Conklin 1	3297.86	137.5	3160.36	166	3,653	3 lb. FL (75% conc.)	3	n.a.	n.a.	n.a.	n.a.	n.a.	n.a.	600 (MG7-11.7)	n.a.	n.a.	30	n.a.	870 @ MG-11	3034	3046	0.2	n.a.	0.031	0.0277	n.a.	n.a.
Aug. 19, 2011	10:50 PM	R. Conklin 2	3297.86	137.5	3160.36	166	3,653	6 lb. FL (75% conc.)	6	30.5	2,874	122.5	716	82.5	1063	n.a.	n.a.	n.a.	30	3.53 @ MG-11	1180 @ MG-11	3034	3046	0.2	0.88	0.031	0.0277	4572	5159
Nov. 18, 2012	2:09 PM	N. Victor 1	3363.55	205	3158.55	243	16,350	14 lb. FL (75% conc.)	14	n.a.	n.a.	n.a.	n.a.	n.a.	n.a.	1200 (estimated MG16-3)	n.a.	n.a.	110 (estimated)	0.3 @ MG-12	468 @ MG-14	3031	3046	0.2	n.a.	0.007	0.0063	n.a.	n.a.
Nov. 4, 2013	2:45 PM	N. Victor 2	3363.55	203.71	3159.84	243	16,350	21 lb. FL (75% conc.)	21	696	564	Forthcoming	Forthcoming	1848	212	Forthcoming	Forthcoming	Forthcoming	Forthcoming	0.55 @ MG-12	Forthcoming	3031	3046	0.2	Forthcoming	0.007	0.0064	6099	6687
Dec. 13, 2012	11:29 AM	Ashmead 1	3240.20	97.00	3143.20	147	2,170	2 lb. FL (75% conc.)	4	17.5	2,976	n.a.	n.a.	31.5	1653	600 (CL300-401)	n.a.	n.a.	5	6 @ CL-404	1120 @ CL-400	3056	3078	0.2	n.a.	0.030	0.0185	n.a.	n.a.
Jan. 31, 2013	12:35 PM	Ashmead 2	3240.20	95.50	3144.70	147	2,170	1 lb. FL (75% conc.)	4	17	3,064	40	1302	32.5	1602	n.a.	n.a.	n.a.	5	2.61 @ CL-404	n.a.	3056	3078	0.2	0.49	0.031	0.0192	8472	13551
Oct. 25, 2013	10:57 AM	Ashmead 3	3240.20	95.70	3144.50	147	2,170	0.5 lb. (75% conc.)	4	17	3,064	38.5	1353	32	1628	n.a.	n.a.	n.a.	4	1.35 @ CL-404	n.a.	3056	3078	0.2	0.49	0.031	0.0191	8828	14147
Nov. 14, 2013	3:16 PM	Strickland 1	3267	60.89	3206	108	18,500	6 lb. FL (75% conc.)	6	576	771	n.a.	n.a.	792	561	5,000	13,000	n.a.	63	0.105@Briggs spr.	Forthcoming	3093	3093	0.2	1.06[a]	0.006	0.0048	18356	23571
Stearns, Harold (USGS 1936)													750																

a = used dominant flow velocity in calculation

b = estimated

*This table of data was updated Feb. 12, 2014 and data presented earlier is superseded by this information. It is up to the user to evaluate for significant digits.